



## **PREPARATION AND CHARACTERIZATION OF SYNTHETIC HYDROXYAPATITE FROM FISHBONE WASTE**

This report is submitted in accordance with requirement of the University Teknikal Malaysia Melaka (UTeM) for Bachelor Degree of Manufacturing Engineering (Hons.)



**FASIHATUNNISA BINTI ABDUL JABAR**

FACULTY OF MANUFACTURING ENGINEERING

2021

## DECLARATION

I hereby, declared this report entitled “Preparation and Characterization of Synthetic Hydroxyapatite from Fishbone Waste” is the result of my own research except as cited in references.

Signature

: .....

Author's Name

: FASIHATUNNISA BINTI ABDUL JABAR

Date

: 25 January 2021



اونيورسيتي تيكنيكل مليسيا ملاك

UNIVERSITI TEKNIKAL MALAYSIA MELAKA

## APPROVAL

This report is submitted to the Faculty of Manufacturing Engineering of Universiti Teknikal Malaysia Melaka as a partial fulfilment of the requirement for Degree of Manufacturing Engineering (Hons). The member of the supervisory committee is as follow:



.....  
(ADIBAH HANEEM BINTI MOHAMAD DOM)



## ABSTRAK

Tulang ikan mempunyai bahan komposit seperti HA berkarbonat, kolagen jenis 1, protein bukan kolagen dan air yang mudah didapati di seluruh dunia sebagai sumber hidroksiapatit semula jadi (HA). HA terkenal dengan sifat biokompatibiliti yang sangat baik kerana mempunyai komposisi kimia yang serupa dengan tisu manusia. Beberapa tahun kebelakangan ini, banyak kajian telah dilakukan untuk mensintesis HA untuk aplikasi dalam biobahan. Oleh itu, kajian ini melaporkan penggunaan sisa tulang ikan (*Skipjack tuna*) untuk membentuk HA menggunakan kaedah kalsinasi pada suhu antara 800°C hingga 1000°C. Semua sampel telah menjalani pencirian fizikal, kimia dan mekanikal untuk memerhatikan morfologi permukaan, penghabluran, kumpulan berfungsi dan kekerasan. Pembelauan Sinar-X digunakan untuk memerhatikan pengaruh suhu kalsinasi pada komposisi fasa HA ketika HA yang dikalsinasi stabil pada 1000°C kerana corak menunjukkan pantulan utama HA dan pantulan CaP yang lebih sedikit, sementara struktur ikatan molekul yang dibentuk oleh HA dihasilkan menggunakan Fourier transform infrared (FTIR) spektroskopi menunjukkan fosfat dan sedikit puncak karbonat dalam sampel yang dirawat. HA yang dihasilkan dari suhu sintesis yang berbeza mempunyai ukuran kristal 44.91-63.17 nm yang dikenal pasti menggunakan persamaan Scherer. Kekerasan HA juga ditentukan oleh penguji kekerasan Vickers, menunjukkan nilai kekerasan tertinggi 0.64 GPa pada suhu 1000°C, yang mana nilai kekerasan berada dalam jarak tulang kortikal femoral manusia yang sebenar. Struktur mikro dan morfologi HA dalam keadaan terkumpul ditentukan dengan menggunakan Mikroskop elektron imbasan. Apabila suhu kalsinasi meningkat, zarah HA membentuk zarah yang padat dan mengakibatkan peningkatan ukuran zarah. Ia dapat disimpulkan bahawa 1000°C dicapai sebagai suhu kalsinasi yang sesuai dengan masa yang tetap bagi tulang ikan untuk membentuk hidroksiapatit.

## ABSTRACT

Fishbone is a composite material made of carbonated HA, type 1 collagen, non-collagen protein and water that is available worldwide as a source of hydroxyapatite (HA). HA was known for its excellent biocompatibility properties due to the similar chemical composition of human hard tissues. Recent years, extensive research and studies have been conducted to synthesise HA for applications in biomaterials. Therefore, this study reported the use of fishbone waste (*Skipjack tuna*) to form HA using calcination method at temperatures ranging from 800°C to 1000°C. All samples have undergone physical, chemical and mechanical characterisation in order to observe surface morphology, crystallinity, functional group and hardness. X-ray diffraction is used to observe the influence of the calcination temperature on the HA phase composition where the calcined HA was stable up to 1000°C because the pattern shows major HA-corresponding reflections and fewer CaP-reflections, while the molecular bond structure formed by HA was produced using Fourier transform infrared spectroscopy (FTIR) demonstrates the phosphate and few carbonate peaks in the sample treated. HA produced from different synthesis temperatures has a crystal size of 44.91-63.17 nm identified by Scherer equation. The hardness of the HA was also determined using the Vickers hardness tester, which showed the highest hardness value of 0.64 GPa at 1000°C, where the hardness value is within the range of the actual human femoral cortical bone. The microstructure and morphology of HA in agglomerated condition was determined using a scanning electron microscopy. As the calcined temperature increases, the HA particle formed a dense particle and resulted in increased particle size. It is concluded that 1000°C is attained as suitable calcination temperature with constant time for fishbone to obtain synthetic hydroxyapatite.

## DEDICATION

I dedicate this research report to  
my father, Abdul Jabar bin Tomin  
my mother, Sakinah binti Hussein  
my sisters and brother,

Thank you for your loving support of my dream and supporting me during my hard time.



## **ACKNOWLEDGEMENT**

### **By the Name of Allah, the Most Merciful and Gracious**

I am using this opportunity to express my deepest gratitude and special thanks to my supervisor, Madam Adibah Haneem binti Mohamad Dom who despite being extraordinarily busy with her duties, took time out to hear, guide and keep me on the correct path throughout this semester and allowing me to carry out the project at their esteemed organisation. Therefore, I consider myself as a very lucky individual as I have the opportunity of associating with her.

I am also very grateful to our assistant engineers who helped me set up the project and gave me practical insights. It is my radiant sentiment to place on record my best regards, deepest sense of gratitude to my family for their careful and precious guidance which were extremely valuable for my study both theoretically and practically. Not forgetting the panels, my friends and the people who helped, supported and contributed to the completion of this research.

I perceive this research as a big milestone in my career development. I will strive to use gained skills and knowledge in the best possible way and I will continue to work on their improvement, to attain desired career objectives.

# TABLE OF CONTENTS

<b>ABSTRAK</b> .....	<b>i</b>
<b>ABSTRACT</b> .....	<b>ii</b>
<b>DEDICATION</b> .....	<b>iii</b>
<b>ACKNOWLEDGEMENT</b> .....	<b>iv</b>
<b>TABLE OF CONTENTS</b> .....	<b>v</b>
<b>LIST OF TABLES</b> .....	<b>viii</b>
<b>LIST OF FIGURES</b> .....	<b>ix</b>
<b>LIST OF ABBREVIATIONS</b> .....	<b>xi</b>
<b>LIST OF SYMBOLS</b> .....	<b>xii</b>
<b>CHAPTER 1: INTRODUCTION</b>	
1.1 Background of study .....	1
1.2 Problem Statement .....	3
1.3 Objectives .....	4
1.4 Scope of the Research.....	4
<b>CHAPTER 2: LITERATURE REVIEW</b>	
2.1 Biological Apatite .....	5
2.1.1 Characterisation of biological apatite.....	6
2.1.2 Substitution of hydroxyapatite .....	7
2.2 Overview of Hydroxyapatite .....	8
2.2.1 Structure of hydroxyapatite .....	9
2.2.2 Properties of hydroxyapatite .....	11
2.2.3 Application of hydroxyapatite.....	11
2.3 Methods of Synthesis Hydroxyapatite .....	12
2.3.1 Dry method.....	12
2.3.2 Wet method .....	13



2.3.3	Hydrothermal method .....	15
2.3.4	Combination method .....	16
2.4	Characterisation of Hydroxyapatite .....	17
2.4.1	X-ray diffraction.....	17
2.4.2	Fourier transform infrared spectroscopy .....	18
2.4.3	Vickers hardness tester.....	18
2.4.4	Scanning electron microscopy .....	19
2.4.5	Particle size analyser .....	20
2.5	Natural Hydroxyapatite.....	20
2.5.1	Extraction of hydroxyapatite from natural sources .....	22
2.6	Overview of Fish .....	24
2.6.1	Production of Tuna fish in Malaysia.....	24
2.6.2	Synthesis of fishbone-based hydroxyapatite.....	26
2.6.3	Characterisation of fishbone.....	27
<b>CHAPTER 3: METHODOLOGY</b>		
3.1	Overview.....	29
3.2	Materials and Equipments .....	29
3.3	Experimental.....	31
3.3.1	Preparation of fishbone powder .....	31
3.3.2	Preparation of synthetic HA pellet.....	32
3.3.3	Characterisation of synthetic HA .....	32
<b>CHAPTER 4: RESULT AND DISCUSSION</b>		
4.1	Observation of Raw Fishbone.....	35
4.2.1	General overview .....	35
4.2.2	X-ray diffraction analysis (XRD).....	36
4.2.3	Fourier-transform infrared spectroscopy (FTIR) .....	37
4.2.3	Synthetic HA pellet analysis .....	39
4.2	Characterisation of Synthetic HA Analysis from Fishbone.....	40
4.2.1	X-ray diffraction analysis (XRD).....	40

4.2.2	Fourier-transform infrared spectroscopy (FTIR) .....	42
4.2.3	Vickers hardness study.....	44
4.2.4	Scanning electron microscopy (SEM).....	45

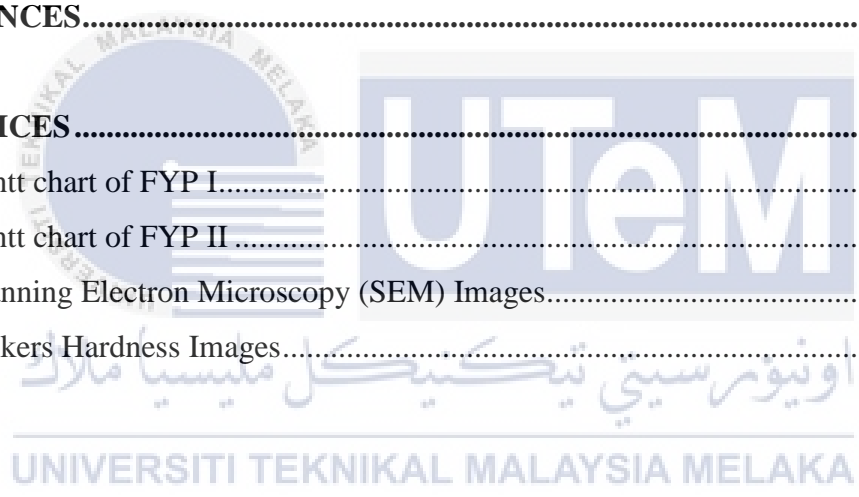
**CHAPTER 5: CONCLUSION AND RECOMMENDATION**

5.1	Conclusion .....	47
5.2	Recommendation .....	48
5.3	Sustainability Element .....	48
5.4	Life Long Learning Element.....	49
5.5	Complexity Element .....	49

<b>REFERENCES.....</b>	<b>50</b>
------------------------	-----------

<b>APPENDICES.....</b>	<b>60</b>
------------------------	-----------

A	Gantt chart of FYP I.....	60
B	Gantt chart of FYP II.....	61
C	Scanning Electron Microscopy (SEM) Images.....	62
D	Vickers Hardness Images.....	64



## LIST OF TABLES

2.1	The properties of crystal structure of HA	6
2.2	Main Calcium Phosphates Group	10
2.3	Methods to prepare HA	17
2.4	Summary method used to extract HA from fishbone	23
2.5	The Amino acid contains in <i>Skipjack tuna</i>	27
3.1	The preparation of fishbone powder	32
4.1	The calcination data of synthetic HA powders at calcined temperatures: 800°C (A800), 900°C (B900), 1000°C (C1000) and commercial HA (C-HA)	36
4.2	FTIR peak value of sample raw fishbone (R-FB)	38
4.3	Physical appearance of sintered pellet at sintering temperature 1000°C	39
4.4	The crystallite size of powder for synthetic HA powders at calcined temperatures: 800°C (A800), 900°C (B900), 1000°C (C1000) and commercial HA (C-HA)	41
4.5	FTIR spectrum observation band positions of synthetic HA powders at calcined temperatures: 800°C (A800), 900°C (B900), 1000°C (C1000) and commercial HA (C-HA)	43
4.6	The Vickers hardness of synthetic HA powders at calcined temperatures: 800°C (A800), 900°C (B900) and 1000°C (C1000)	44

## LIST OF FIGURES

2.1	Unit cell of Hydroxyapatite	10
2.2	The image of HA rods synthesised in hydrothermal reaction by using SEM analysis	15
2.3	The image of HA rods synthesised in hydrothermal reaction by using SEM analysis	16
2.4	Principle of Vickers Hardness Tester	19
2.5	Summary of extracting HA from natural sources	21
2.6	The production of Tuna Fish (Kawakawa and Longtail) in Malaysia (1990-2015) source from Department of Fisheries (DOF) statistics report	24
2.7	The measurement of frozen fish sizes	26
3.1	Schematic flow process chart of preparation and characterisation of HA from fishbone	30
4.1	General observation of raw fishbone (R-FB) and calcined fishbone at calcined temperatures: 800°C (A800), 900°C (B900) and 1000°C (C1000)	36
4.2	XRD pattern analysis of sample raw fishbone (R-FB) compared with sample calcined powder at 800°C (A800)	37
4.3	FTIR spectrum analysis of sample raw fishbone (R-FB) compared with sample calcined powder at 800°C (A800)	38
4.4	XRD pattern analysis of synthetic HA powders at calcined temperatures: 800°C (A800), 900°C (B900), 1000°C (C1000) and commercial HA (C-HA)	41

4.5	FTIR spectrum analysis of synthetic HA powders at calcined temperatures: 800°C (A800), 900°C (B900), 1000°C (C1000) and commercial HA (C-HA)	43
4.6	Hardness with 5 tons compaction pressure analysis of synthetic HA powders at calcined temperatures: 800°C (A800), 900°C (B900) and 1000°C (C1000)	45
4.7	SEM images analysis of synthetic HA powders at calcined temperatures: a) 800°C (A800), b) 900°C (B900), c) 1000°C (C1000), d) Commercial HA (C-HA) at 10,000X	46



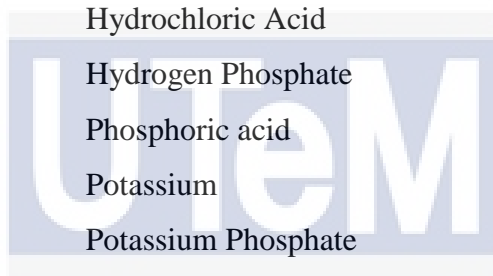
## LIST OF ABBREVIATIONS

ASTM HA	-	American Society for Testing and Materials (Standard HA)
A800	-	Calcined temperature at 800°C
B900	-	Calcined temperature at 900°C
C1000	-	Calcined temperature at 1000°C
C-HA	-	Commercial hydroxyapatite
Cu K $\alpha$	-	Copper K-alpha
DCPA	-	Dicalcium Phosphate Anhydrous
EDX	-	Energy dispersive x-ray
FB	-	Fish bone
FTIR	-	Fourier-transform infrared spectroscopy
FWHM	-	Full width at half maximum
HA	-	Hydroxyapatite
IR	-	Infrared radiation
JCPDS	-	Joint Committee on Powder Diffraction Standards
PSA	-	Particle size analyser
PVA	-	Polyvinyl alcohol
R-FB	-	Raw fish bone
SEM	-	Scanning electron microscope
SST	-	sea surface temperature
TCP	-	Tri-calcium phosphate
TTCP	-	Tetracalcium Phosphate
XRD	-	X-ray diffraction

## LIST OF SYMBOL

$\lambda$	-	Wavelength (Lambda)
$^{\circ}$	-	Degree
$\theta$	-	Angle Diffraction
%	-	Percentage
$^{\circ}/\text{min}$	-	Degree per minute
$^{\circ}\text{C}$	-	Degree Celsius
$\mu\text{m}$	-	Micrometre
$\text{cm}^{-1}$	-	Reciprocal Centimetre
drop/min	-	Drop per minute
g	-	Gram
kgf	-	Kilogram-force
kV	-	Kilovolt
mA	-	Milliampere
mm	-	Millimetre
nm	-	Nanometre
pH	-	Potential of Hydrogen
psi	-	Pound per square inch
rpm	-	Revolution per minute
GPa	-	Giga Pascal
M	-	Moles
MPa	-	Mega Pascal
X	-	Magnification
$\beta$ -TCP	-	$\beta$ - Tricalcium Phosphate
Al	-	Aluminum
$\text{AlO}_2$	-	Aluminum Oxide
Ba	-	Barium
C-H	-	Carbon hydrogen bond

C-N	-	Carbon nitrogen bond
C=O	-	Carbon oxygen double bond
C-C	-	Carbon carbon bond
C-O	-	Carbon oxygen bond
CO <sub>2</sub>	-	Carbon dioxide
CO <sub>3</sub> <sup>2-</sup>	-	Carbonate
Ca	-	Calcium
CaO	-	Calcium Oxide
CaCO <sub>3</sub>	-	Calcium Carbonate
Ca(OH) <sub>2</sub>	-	Calcium hydroxide
CaP	-	Calcium Phosphate
HCl	-	Hydrochloric Acid
HPO <sub>4</sub> <sup>2-</sup>	-	Hydrogen Phosphate
H <sub>3</sub> PO <sub>4</sub>	-	Phosphoric acid
K	-	Potassium
KH <sub>2</sub> PO <sub>4</sub>	-	Potassium Phosphate
Mg	-	Magnesium
Na	-	Sodium
NH <sub>4</sub> OH	-	Ammonium hydroxide Solution
OH-	-	Hydroxide
OH	-	Hydroxyl
Pb	-	Lead
PO <sub>4</sub> <sup>3-</sup>	-	Phosphate
Si	-	Silicon
Sr	-	Strontium
Ti	-	Titanium
Zr	-	Zirconium



اونيورسيتي تيكنيكل مليسيا ملاك  
UNIVERSITI TEKNIKAL MALAYSIA MELAKA



# CHAPTER 1

## INTRODUCTION

### 1.1 Background of Study

Hydroxyapatite (HA) or known as synthetic HA is specifically found in the form of granular particles, porous blocks, powder and different sintered form as a source of calcium for teeth and important compounds to repair bones described by Afriani *et al.* (2019). The molecular formula of HA is  $\text{Ca}_5(\text{PO}_4)_3\text{OH}$  but frequently written as  $\text{Ca}_{10}(\text{PO}_4)_6(\text{OH})_2$  (Pokhrel, 2018). The material is one of the most important minerals in the group calcium phosphate (CaP). CaP was found in bone basically in the form of a nanometre-sized needle of crystals. However, it has a poorly crystallized non-stoichiometric apatite phase (Gomes *et al.*, 2019). Dynamically, Ghiasi *et al.* (2019) stated that HA is the most stable based on physiological conditions as compared to other CaP compounds. Hence, HA is focusing on biomedical applications with properties closer to living organisms. Based on chemical properties, synthetic HA is a rare material due to high bioactivity, high biocompatibility and non-toxicity of bone and tooth in living organisms, which is not harmful to the body (Martin *et al.*, 2019).

The application enhances from HA has been applied widely in industries which, for example, replacement concretes material, fertilizer activities, limestone agent and production of tile. HA extracted from chemical synthesis have been intensively studied in recent years. However, the study of use natural sources has recently increased. Recently, many researchers reported that HA from natural sources specifically fishbone has excellent potential in health applications that used as a biomaterial for bone implant (Mustafa *et al.*, 2015; Shi *et al.*, 2018; Pu'ad *et al.*, 2019). Indeed, HA compound from fishbone has been used as human body implant materials such as prosthetic implants and coating (Pokhrel, 2018; Khiri *et al.*, 2019).

The aquaculture industry is one of the leading industry and eventually to become the source of Malaysia's economy. Consequently, Malaysia is known as a maritime nation because of the strategic location with an abundant supply of land and water suit to aquaculture activities. Fish is known as one of the primary protein sources that can be found easily from aquaculture activities. There are 22,000 known species of fish in global. *Skipjack tuna* is one of the species which known as *Katsuwonus pelamis* is a perciform fish in the tuna family. The major increase in tuna landings was due to the expansion of commercial tuna fishing of Malaysia's exclusive economic zone (EEZ) waters, especially around the South China Sea. It is expected that the production of tuna in Malaysia will continue to show significant growth in the future. With a growing population of people, the estimation of the annual demand for fishes will increase. Thus, the need for fishes has increased the amount of fish waste specifically fishbone. Fishbone is a composite material made of carbonated HA, type 1 collagen, non-collagenous protein and water. It is available in worldwide, low-cost source to obtain natural HA (Shi *et al.*, 2018). Many research have been carried to reuse waste bones for both environmental and economic benefits.

Many researchers have studied the method to synthesise HA. HA can be synthesised in various ways such as dry method, wet chemical precipitation reaction and hydrothermal technique (Khandelwal and Prakash, 2016). The alkaline method is able to produce pure HA, but with lower crystallinity as compared to the calcination method. In addition, the alkaline method is one of the expensive preparation technique used by the laboratory to synthesize HA is limited because it requires a large quantity of material to form it. Therefore, the method of synthesising HA is crucial to the production of pure HA with high crystallinity. The preparation of synthetic HA with specific characteristics remains challenging for every researcher due to the possibility of developing toxic products during the synthesis process (Pu'ad *et al.*, 2019). Thus, this research is focusing on synthesised and characterised synthetic HA from fishbone powder by using x-ray diffraction (XRD), Fourier-transform infrared spectroscopy (FTIR), Vickers hardness tester and the scanning electron microscopy (SEM).

## 1.2 Problem Statement

Bone is a skeleton organ system known as calcified tissue that protects soft tissues and organs, provides the body with a mechanical support and restores mineral homeostasis. Bone consists of approximately 60% of minerals with hydroxyapatite (HA) being one of the mineral phases, 30% of organic by mass and 10% of water. Recent years, HA is well known for bone regeneration through conduction or by acting as a scaffold for repairing the defects. As a consequence, HA plays a significant role in bone replacement or bone tissue regeneration. Due to the limited supply of natural bones for bone replacement, there is a growing need for synthetic bones to replace bones with the same biological properties as natural bones. This has given rise to importance in the development of artificial materials as bone graft substitutes.

There have been increasing research and development activities of HA due to its high demand as a promising biomaterial. One of the factors contributing to the increase in the global stoichiometric HA market is the excessive applicability of HA in the medical sector. Additionally, the demand for HA in dental implants is predicted to increase over the forecast period (Thirumalai, 2018). Nevertheless, the low mechanical properties of HA are expected to restrain market growth. In order to reduce the dependency on stoichiometric HA materials for industries, efforts have been made to incorporate by-products and wastes from different natural sources as alternatives in obtained HA. Therefore, fishbone currently is found to be the best candidate as the alternative material as they lead to the best results producing HA (Pu'ad *et al.*, 2019). The formation of HA using fishes waste can be reduced the production cost and the price of HA in the global market. Waste should be recycled and reused toward the production of value-added products to sustain product development. Previous studies by Venkatesan *et al.* (2015) have generally focused on the thermal method of synthesising HA from the fishbone to form HA. However, it was found that the presence of tricalcium phosphate (TCP) phase at 1200°C. Hence, the calcination temperature is crucial to the production of HA. This study focuses on the use of fishbone waste (*Skipjack tuna*) as a source for the synthesis and characterisation of highly pure HA powder. This research will help meet the objective by raising awareness of possible ways to develop economic return from natural waste, especially in fishbone.

### 1.3 Objectives

The objectives of this study are as follows:

- a) To synthesise hydroxyapatite powder from fishbone via calcination method.
- b) To characterise and analyse the physical, chemical and mechanical properties of fishbone.
- c) To investigate the suitable calcination temperature with constant time for fishbone to obtain hydroxyapatite.

### 1.4 Scope of the Research

The scopes of research are as follows:

- a) Study the physical properties of fishbone via the purification process and dried in oven for one hour. The amount of fishbone powder was prepared by crushing it into small parts and go through the pulverizing process.
- b) Identify the best amount of fishbone for the preparation of three samples that were subjected in the sintering process which all samples in three different condition temperatures of thermal method.
- c) Investigate the best temperature that produces synthesis HA from fishbone, which identified via the X-ray diffraction (XRD) and Fourier-transform infrared spectroscopy (FTIR).
- d) Observe the effect shape of the HA particles in different synthetic temperature in considering the crystallinity of HA powders and improved synthesis method to produce HA from fishbone.

## **CHAPTER 2**

### **LITERATURE REVIEW**

This chapter consists of two sections that explored the theory and experimental work performed by different researcher years ago. Related knowledge from previous studies refers to the book and some source of internet relevance to the scope of the study included background of natural hydroxyapatite and characterisation techniques.

#### **2.1 Biological Apatite**

Biological apatite is known as inorganic calcium phosphate (CaP) has many characteristics differing either from mineral apatite or synthetic apatite while Vallet-Regí (2016); Siddiqi and Azhar (2020) said that biological apatite specifically in human bone is containing 4 to 8 weight% of carbonate ion in lattice substitutions which occur in two groups known as A-site for hydroxyl ion and B-site for phosphate ion. It is found as apatite structure, but some of crystallized CaP phases (Whitlockite, Brushite and Octacalcium Phosphate) may form in unknown pathologic clarifications. CaP is stated as one of the essential minerals for both bones (skeletal system and homeostasis of mineral balance in body) and teeth (Upadhyay, 2017). CaP has been performed as filler in biological tissues where it is important to the physicochemical characteristic of any materials. Haider *et al.* (2017) reported that biological apatite structure is identical to the tissues present in the bone which is bioactive and applied as a substitute for the bone construction in periodontology, oral as well as orthopaedic processes. The bones were used for the reconstruction of the bone defect. Biological apatite is an excellent mineral dependent on structure and work in and applications of biological tissues which many researcher had performed the investigation of its physicochemical and biological properties (Eliaz and Metoki, 2017; Kołodziejaska *et al.*, 2020).

### 2.1.1 Characterisation of biological apatite

Based on chemical characterisation, biological apatite is regarded as HA which the result of CaP performed in apatite structure. CaP capable to absorb proteins into biomaterial surfaces that give benefit for tissue or material interface, which leading to expanded bone formation (Neacsu *et al.*, 2019). Among the apatite family, HA is the best material for improving any application involved. HA is known as one of the apatite family that plays a significant role in the biomaterials field (Haider *et al.*, 2017). From the previous research of Liu *et al.* (2013), they showed the composition and structure of HA which two different crystals formed had investigated known as hexagonal with the lattice parameters (Hexagonal HA) and monoclinic with the lattice parameters (Monoclinic HA). They found that both had the same elements and stoichiometric Ca/P ratio of 1.67. Besides, the direction of hydroxyl (OH) group is the main difference that occurs in their structure. For Hexagonal HA, the OH groups formed in the reverse directions, while for Monoclinic HA, the OH groups have the same direction among themselves (Saxena *et al.*, 2018). Table 2.1 below shows the properties of the crystal structure of HA which described the summary of both elements.

Table 2.1: The properties of crystal structure of HA (Saxena *et al.*, 2018)

Properties	Hexagonal	Monoclinic
Symmetry	P6 <sub>3</sub> /m	P2 <sub>1</sub> /b
Lattice parameter	a= b=9.432Å c= 6.881Å γ=120°	a=9.4214Å b=2a, c=6.8814 Å γ=120°
Orientation of Hydroxyl groups (OH)	Reversed direction.	Same direction.

For this reason, biological apatite basically is Ca/P minerals incorporated by various type of ions which is Calcium (Ca), Phosphorus (P) and Oxygen (O) are three major elements composing the Ca/P minerals. Carbon (C), Sodium (Na), Potassium (K), Fluorine (F), Magnesium (Mg), Aluminium (Al), Strontium (Sr), Chloride (Cl) and other elements also found as incorporated ions in the biological apatite structure which then influence the stability of biological apatite (Laskus and Kolmas, 2017). Their present may differ among sources which all the elements stated may be found in small amounts in biological apatite structure. Eliaz and Metoki (2017) reported that the Ca/P ratio of biological apatite was either

lower than the Ca/P ratio of stoichiometric HA or close to the Ca/P ratio of stoichiometric HA which state as 1.67 based on research by Elliott (2013). However, the Ca/P ratio of biological apatite would be higher than Ca/P ratio of stoichiometric HA which different from the statement mentioned from Barakat *et al.* (2008). This statement may lead to the difference testing method, raw materials as well as detection error. The difficulty of evaluating chemical compositions is due to the ion absorptions. The effect on each crystal may be distinctive, which the structure of apatite allows for wide compositional variations due to the ability in obstruct different ions in different conditions (Eliaz and Metoki, 2017). In physiological characterization, CaP is partially dissolved caused by cellular activities and will increased the biological or physiological fluid. There are two aspect that biological apatite shows the unique chemical composition. The first aspect is the lacking of anticipatory hydroxyl group while second aspect is the existence of  $\text{HPO}_4^{2-}$ . It was reported by Liu *et al.* (2013) that hydroxyl group have only a least amount concentration detected in bone. It is because the multiple ionic substitutions which often occur in the lattice of biological apatite.

Other than that, the existence of  $\text{HPO}_4^{2-}$  also could be occur due to the ionic substitutions. However, due to the lack of accuracy of the analytical method, it is impossible to measure the number of chemical groups accurately. The external factor that can influenced the chemical groups were temperature, inorganic solvent, ionic effect and the pH scale. Biological apatite might lose carbonate groups by sintering it in temperature of  $850^\circ\text{C}$  for two hours who was observed by Liu *et al.* (2013). This can cause a partial dissolution of biological apatite crystals for inorganic solvents such as acid and pure water. Based on crystal structure analysis, Liu *et al.* (2013) said that the biological apatite crystal size may reach more than 100 nm. They believed that the size of crystal as well as age of crystal highly depends on the age of mammal's bone. Kaflak *et al.* (2019) approved the statement in their research where they noticed a decrease in the percentage of amorphous minerals in rats from 69% to 36% when the animal age rose from five to 70 days.

### **2.1.2 Substitution of hydroxyapatite**

In actual fact, biological apatite behaviour has been investigated since ages ago which then the researcher namely Horvath derived the solubility of this apatite specifically from bones and teeth (Horvath, 2006). Based on the research, the result of the solubility of



biological apatite was missing as it needs more accurate data of solubility biological apatite. After all, the research from Zhuofan *et al.* (2009) had proved that the solubility of bovine bone which known as a cattle of group (Bio-Oss) shows that HA consists in its bone was naturally higher than synthetic HA which may lead to the bad effect of the crystallinity of synthetic HA than the biological apatite. However, Liu *et al.* (2013) revealed that Mg consists of biological apatite was causing to the high solubility in biological apatite. In conclusion, the result of solubility for biological apatite is remain unanswered.

Biological apatite performance of bone development and implants are highly depends on positive interaction with human body and the surrounding of tissues specifically after the implantation process. The cation substitution of HA might prove the significance of the biomedical field as it needs to be emphasized which they could lead the road toward an upgrade generation of implant coatings in the medical field. From this reason, biological apatite is known as CaP which very similar to the Hydroxyapatite ( $\text{Ca}_{10}(\text{PO}_4)_6(\text{OH})$ ) and is considered to be the major component of the mineralized part of bone.

## 2.2 Overview of Hydroxyapatite

Upadhyay (2017) derives HA as a natural mineral form of calcium apatite which consists of calcium, phosphorus and oxygen in CaP group. HA can be crystallized in the shape of hexagonal crystals which usually found in white colour. In the middle of the 18<sup>th</sup> Century, the researcher starts to investigate the chemical structure and composition of the CaP compound. Fortunately, in the 19<sup>th</sup> Century, the CaP group existed in different phases which in the earlier Century all CaP were called as apatite as reported by Haider *et al.* (2017). HA is mainly important among the various CaP group because of its structural and chemical very similar to the main mineral component in human bone. Hence, HA has been widely used especially in the science field. In fact, Khandelwal and Prakash (2016) stated that human bone in the category of an adult consists of 70% inorganic elements and 30% other organic elements which is collagen. The major minerals component composed of HA (insoluble salt of calcium and phosphorus). Based on chemical analysis, the bone consists of a large number of complex groups which is cations and anions such as Calcium (Ca), Phosphorus (P) and Carbonate ( $\text{CO}_3^{2-}$ ). However, bone also consists of a small amount of Magnesium (Mg), Iron (Fe), Fluorine (F) and Chlorine (Cl). When the cellular exchange,



Sodium (Na) and Potassium (K) also found but in small amounts and heavy atoms such as Barium (Ba), Strontium (Sr) and Lead (Pb).

Moreover, Khandelwal and Prakash (2016) explained two ions in HA provides the formation of salts which is calcium and phosphorus, especially amorphous HA and calcium triphosphate in organic elements. Meanwhile, in inorganic elements, when the structure of HA has been crystallized, it is called as practically HA. It provides the mechanical features of the bone. Hence, it is mainly important the study of natural mineral form as potential bone substitutes and in particular CaP which is HA.

### 2.2.1 Structure of hydroxyapatite

Generally, HA molecular formula stated as  $\text{Ca}_5(\text{PO}_4)_3\text{OH}$ , but frequently written as  $\text{Ca}_{10}(\text{PO}_4)_6(\text{OH})_2$  (Pokhrel, 2018). Haider *et al.* (2017) proved that atomic structure of HA consists of Calcium ions  $\text{Ca}^{2+}$  and surrounded by Phosphite ions  $\text{PO}_4^{3-}$  as well as hydroxyl ions  $\text{OH}^-$ . Gomes *et al.* (2019) analysed that there are 39% by weight of Ca, 18.5% P and 3.38%  $\text{OH}^-$ . Besides, the molar ratio of HA in CaP is 1.67. They identified the essential compounds of calcium phosphate by referring to the increasing molar rate of CaP.

Based on the list of the CaP compounds in table 2.2, the higher the CaP ratio, the less a compound's solubility. The exception is the compound with the highest CaP ratio is TTCP, which have the highest solubility in the CaP group. Meanwhile, Haider *et al.* (2017) research revealed the neutral pH is mainly important to the body temperature. This is because both of these materials are embedded in the human body has a near-neutral pH value. Thus, the highest acidity and basicity will trigger the soft tissues in our body. Wagh (2016) proved that the most stable compound in near-neutral pH is HA which found in the main bone component. Additionally, Gomes *et al.* (2019) agreed TTCP is the only compound which has the largest CaP ratio in Table 2.1. However, TTCP is the only compound that can react to form HA with another CaP group having a lower CaP ratio. Thus, the TTCP and DCPA reaction should produce HA without adding any acidity and basicity to the soft tissues in our bones.

Table 2.2: Main Calcium Phosphates Group (Szcześ *et al.*, 2017)

Ca/P	NAME	SYMBOL	FORMULA
0.5	Monocalcium Phosphate Monohydrate	MCPM	$\text{Ca}(\text{H}_2\text{PO}_4)_2 \cdot \text{H}_2\text{O}$
0.5	Monocalcium Phosphate Anhydrous	MCPA	$\text{Ca}(\text{H}_2\text{PO}_4)_2$
1.0	Dicalcium Phosphate Dihydrate	DCPD	$\text{Ca HPO}_4 \cdot 2\text{H}_2\text{O}$
1.0	Dicalcium Phosphate Anhydrous	DCPA	$\text{Ca HPO}_4$
1.33	Octacalcium Phosphate	OCP	$\text{Ca}_8 (\text{HPO}_4)_2 (\text{PO}_4)_4 \cdot 5\text{H}_2\text{O}$
1.5	$\alpha$ -Tricalcium Phosphate	$\alpha$ -TCP	$\alpha\text{-Ca}_3 (\text{PO}_4)_2$
1.5	$\beta$ -Tricalcium Phosphate	$\beta$ -TCP	$\beta\text{-Ca}_3 (\text{PO}_4)_2$
1.2-2.2	Amorphous Calcium Phosphate	ACP	$\text{Ca}_x (\text{PO}_4)_y \cdot n\text{H}_2\text{O}$
1.5-1.67	Hydroxyapatite Deficient In Calcium	CDHA	$\text{Ca}_{10-x}(\text{HPO}_4)_x (\text{PO}_4)_{6-x}(\text{OH})_{2-x}$ ( $0 < x < 1$ )
1.67	Hydroxyapatite	HA or HAp	$\text{Ca}_{10}(\text{PO}_4)_6 (\text{OH})_2$
2.0	Tetracalcium Phosphate	TTCP	$\text{Ca}_4 (\text{PO}_4)_2 \cdot \text{O}$

Jang *et al.* (2015) described there are two CaP materials that are stable at room temperature with comfortable ambient temperature, 20°C when contact with body fluids. The pH value can be used to determine the stability of CaP material. The pH value lower than 4.2 is DCPD ( $\text{CaHPO}_4 \cdot 2\text{H}_2\text{O}$ ). While pH value greater than 4.2 is HA ( $\text{Ca}_{10}(\text{PO}_4)_6(\text{OH})_2$ ). In addition, HA has a simple crystallographic structure and composition based on unit cell reproduction in figure 2.1. The symmetry of the hexagon and the cell lattice structure and its symmetry is known as the unit cell along the c-axis. This will justify a preferential orientation that leads to a c-axis and a morphology like needles (Sahu *et al.*, 2012).

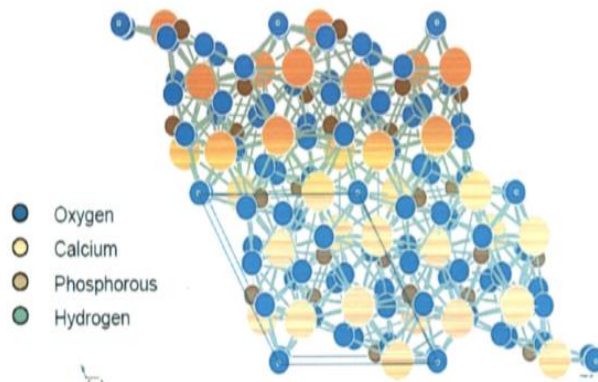


Figure 2.1: Unit cell of Hydroxyapatite (Sahu *et al.*, 2012)

### 2.2.2 Properties of hydroxyapatite

Research by Lin and Chang (2015) proved that HA has low mechanical properties and agreed by Veljović *et al.* (2013) stated that the fracture toughness of HA is less than  $1\text{MPa m}^{1/2}$ . Thus, it needs to increase its mechanical stability. As a result, research has been performed to determine the behaviour of HA doped with a variety of strengthening agents for example at different oxides (Titanium (Ti), Zirconium (Zr), Magnesium (Mg) or Aluminium Oxides ( $\text{AlO}_2$ )). Unfortunately, the finding show that bioactivity and biocompatibility have significantly decrease. The deterioration rate, linked to its durability is contributes to the difficult resorption of human body is also identified as another issue of HA reported by Hickey *et al.* (2015). For bone tissue engineering application, the controlled degradation rate is important, therefore, HA composite is considered a viable alternative as it can manufacture with the introduction of second phase with a higher rate of degradation.

HA is very biocompatible with the human body and has a similar mineral composition in the bone. HA is osteoconductive, bioactive and has no negative effect on the human body. Due to the unique features, HA has attracted a large number of researchers to research on HA as a substitute for bones. Due to its biocompatibility HA in dentistry and orthopaedics which has been success used for several years, it will established a strong bond when implanted into the human body (Nawang *et al.*, 2019). However, Ramesh *et al.* (2018) reported that some drawbacks do exist for HA derived from the synthetic route. The negative aspects include costly starting materials because of warranted ultra-high-purity chemicals, such as the removal of unnecessary by-product chemical compounds after HA synthesis. There was also a lack of other elements, for example Na, Si, Fe or carbonate.

### 2.2.3 Application of hydroxyapatite

HA is known as  $\text{Ca}_{10}(\text{PO}_4)_6(\text{OH})_2$  is similar to the bone and teeth mineral portion with high biocompatibility, bioactivity, and osteoconductivity properties. This will generate a broad range of applications, particularly in biomedicine field (Lin and Chang, 2015; Haider *et al.*, 2017; Szcześ *et al.*, 2017). Basirun *et al.* (2018) mentioned that HA ceramics are used in bone substitutes for bone-replacement grafting with the interconnected porous system. The implanted material was not incompatible or rejected. On the metallic substrate as a plate,

Asri *et al.* (2016) proposed that HA be applied. The resulting material can maintain biocompatibility in this case, but also show better mechanical properties.

In hard tissue engineering, HA is important because of its excellent biocompatibility and bioactivity compared to other materials. (Haider *et al.*, 2017). Since the 1970s, orthopaedic and dental repair of HA-based biomaterials has been used clinically. Surface modifications on prothesized metal implants with the HA layer are also widely used to improve bone integration. Haider *et al.* (2017) explored the use of Nano rods or nanoparticles for various proteins (growth factors) and drugs, including the use of HA as a carrier for drug delivery. They added an amino acid (glutamic acid) to the surface of HA. The HA Nano rods or nanoparticles modified with a medicament were then mixed with a polymer solution to move HA to the target location.

In addition, environmental applications also used HA as based-biomaterials, such as contaminated soil remediation (Yang *et al.*, 2016), water purification (Alif *et al.*, 2018) and heavy metal adsorption (Zeng *et al.*, 2019) have been exploited.

### **2.3 Methods of Synthesis Hydroxyapatite**

Based on the method used, CaP-based materials with different phases can be permitted resulting in materials with different properties, such as crystalline defects, high surface area located in the physiological part and so on mentioned by Gomes *et al.* (2019). In addition, HA can be synthesized using a number of techniques widely divided into four methods.

#### **2.3.1 Dry method**

Some authors used dry methods such as a solid state reaction and a mechanical alloying process to prepare HA.

Solid state reactions are reactions under conventional heating, which involve high temperatures and high reaction times. Unfortunately, the type of reaction can be accelerated

under microwave heating due to rapid heating, selective bonding and improved kinetic reactions. Microwave energy is used as to process different types of matter including organics, ceramics, polymers, plastics, sol-gel, metals and composites has been massively improved. Rhee (2002) prepared HA by solid-state reaction, but using different chemical reactants,  $\text{Ca}_2\text{P}_2\text{O}_7$  and  $\text{CaCO}_3$ . Both powders have been reused as starting materials and blended respectively into acetone and water. Thus, after heat treatment at  $1100^\circ\text{C}$  in one hour, it will develop single phase HA only in water-melted powder. The results have been explained by the mechano-chemical reaction, which could supply sufficient hydroxyl group to the initial HA in a single phase.

With a mechanical alloying technique, Silva *et al.* (2003) investigated five various testing methods for preparing Nano-crystalline HA specimens in a strictly dry climate. The use of this method did not require heat treatment but required a long frying period up to 60 hours. Rhee (2002) stated that high reproducibility, low manufacturing costs and high crystallinity were supported by the dry chemical synthesized HA in mass production. Meanwhile, he also proposed that dry chemical methods be associated with the possibility of contamination during the milling process.

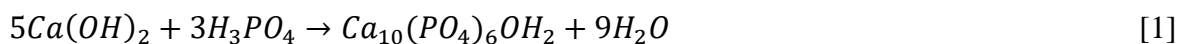
The advantage of using a dry method is the low cost with simple procedure to synthesise HA. High crystalline HA can also be made by this method. It is suitable for mass production of HA where precise controlled conditions are mainly not necessary. However, this dry method specifically for mechanical alloying process will produce low phase purity of HA samples while using solid state reaction can cause large size particles of the samples (Gomes *et al.*, 2019).

### **2.3.2 Wet method**

This method were involve is the low temperature chemical precipitation analysis, co-precipitation analysis, sol-gel route analysis and hydrolysis analysis.

As because the method is easy to operate and need low processing temperatures, Jillavenkatesa and Condrate Sr (1998) indicated that the most widely used technique for HA preparation is known as the precipitation process.  $\text{CaOH}$ ,  $(\text{NH}_4)_3\text{PO}_4$  with  $\text{Ca}(\text{NO}_3)_2$ ,

calcium hydroxide with hydrogen were the typical reactant combinations. On the basis of these combinations, reactions between Ortho-phosphoric acid and calcium hydroxide were proposed as a valuable method of industrial production of HA, since water is the by-product. Equation 1 expresses this chemical reaction revealed by Bigi *et al.* (2007).



Bigi *et al.* (2007) also developed HA crystals using a precipitation method by using  $Ca(NO_3)_2 \cdot 4H_2O$  and  $(NH_4)_2HPO_4$  as a calcium and phosphate ions source. During the synthesis process,  $NH_4OH$  is used to maintain the pH value of solution at 10 while the reacting temperature is retained at  $90^\circ C$  in 5 hours.

Türk *et al.* (2019) mentioned that sol-gel method is also used frequently in preparing HA since it allows control phase formation and purity of the formed phase and processing at low temperatures.  $Ca(NO_3)_2 \cdot 4H_2O$  with  $(C_2H_5O)_3PO$ ,  $Ca(OEt)_2$  with  $(PO(OEt)_3)$ ,  $Ca(NO_3)_2(OH)_2$  and  $Ca(NO_3)_2 \cdot 4H_2O$  with  $P_2O_5$  are all the most commonly used reactants. However, the formed HA material may contain secondary phases such as CaO that have reported negative impacts on HA's biocompatibility. CaO can be transformed into  $CaCl_2$ , which can be extracted by filtering by using HCl (Hsieh *et al.*, 2001; Türk *et al.*, 2019) as a solution to the above problem. Other shortfalls in the approach to sol gel, including high costs for alcohol-based starting materials, complicated steps to complete the dissolution of the starting material and so on have also been mentioned by Santos *et al.* (2004)

As a summary, the use of a wet method to analyse HA samples may provide an accurate result of morphology and size of the particles. It is known as the most promising method of synthesizing HA powder. Even though wet precipitation methods have been widely used (Hsieh *et al.*, 2001; Santos *et al.*, 2004), HA contamination with impurities is likely to lead to the development of non-stoichiometric HA and changes in structural properties and characteristics. Consequently, control the processing parameters such as pH, temperature, reactive concentration during synthesis is very important, as these parameters can lead to changes in crystallinity, morphology and particle size which can influence applications of HA's result (Gomes *et al.*, 2019).



### 2.3.3 Hydrothermal method

This method were involve the aqueous solutions of high temperature and high voltage analysis, emulsion and micro-emulsion and sono-chemical analysis.

In recent years hydrothermal analyses to generate HA significantly improved. Studies have shown that changes in hydrothermal temperature, hydrothermal time and concentration of reactions can regulate HA shape and size (Ma, 2019). The reaction system and conditions for HA preparation are convenient, while the synthesis temperature is relatively low. Hydrothermal treatment is one of the early synthesis methods for HA mixed with Fluroapatite,  $\text{Ca}_{10}(\text{PO}_4)_6\text{F}_2$  under 5000 psi and at 920-1230°C temperatures. Zhang and Vecchio (2007) also tried the hydrothermal procedure by using dicalcium phosphate anhydrous chemical reagents, ( $\text{CaHPO}_4$ , DCPA) and  $\text{CaCO}_3$  at temperatures of 120 to 180°C. The resulting material was HA with a 24 hours reaction temperature of 140°C, but also contain a small amount of  $\beta$ -TCP as to be a by-product. Based on figure 2.2, the HA rods have a morphology of about 200 nm in width and length.

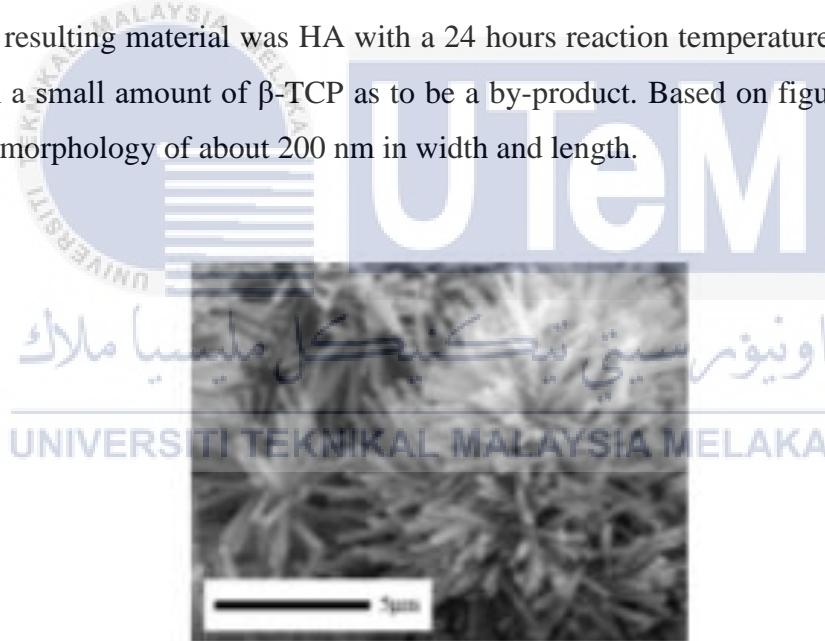


Figure 2.2: The image of HA rods synthesised in hydrothermal reaction by using SEM analysis (Zhang and Vecchio, 2007)

In a hydrothermal reaction at 200°C, within 24 to 72 hours, described by Earl *et al.* (2006), this method used in the heating of precipitate HA, formed by mixing  $\text{Ca}(\text{NO}_3)_2 \cdot 4\text{H}_2\text{O}$  ( $\text{NH}_4$ ). A 24-hour treatment period developed single phase powder by using XRD analysis, although the presence of monetite, secondary phase ( $\text{CaHPO}_4$ ), is shown by XRD trends for longer treatment periods. A SEM analysis showed rod-like morphological particles between 100 and 600 nm in length and also between 10 and 60 nm in diameter as shown in figure 2.3.

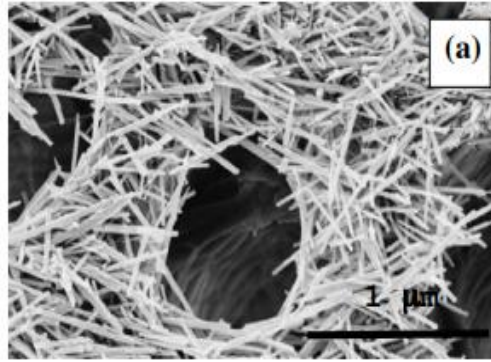


Figure 2.3: The image of HA rods synthesised in hydrothermal reaction by using SEM analysis (Earl *et al.*, 2006)

The advantage of using this method is HA produced usually relatively stoichiometric and high crystalline. However, this treatment requires costly equipment and difficult to control the size and morphology of HA powder (Sadat-Shojai *et al.*, 2011).

#### 2.3.4 Combination method

The combination method is widely used as it can produce approximately close to the ideal CaP ratio which is 1.67. Generally, the extraction HA from natural sources were using combination method as it is hard to examine if the materials are dirty. Hence, the natural sources need to calcine as to remove dirt particle which then will be used chemical precipitation as further treatment to produce high purity HA. Table 2.3 depicts the processing characteristics of each method used for the synthesis of HA particles will vary and lead to different morphologies, as shown in table 2.3. The strength and osteo-integration of powders are crucial features greatly depends on their microstructure. The challenge of synthetic HA is to control the growth of crystals because they may influence the mechanical properties, conditions of processing, surface chemicals, biocompatibility as well as bioactivity based on the distribution of their microscopic form and size. Conventional mechanical and wet chemical methods may allow better control of the stoichiometry at the end of the product. Other stages, such as  $\beta$ -TCP and CaO, may be formed if CaP stoichiometry during precipitation is not adjusted at 1.67. Biomedicine applications require accurate testing of particle size and morphology, porosity and a surface area, which are important features to ensure biological system reactivity and interaction.



Table 2.3: Methods to prepare HA (Gomes *et al.*, 2019)

Method	Type	Temp.	Morphology	Purity	Particle size
Dry method	Solid state reaction	1000°C	Miscellaneous	Low	Micron
	Mechanical alloying	1000°C	Miscellaneous	Low	Nano
Wet method	Chemical precipitation	100-1300°C	Miscellaneous	Variable	Most Nano-sized
	Sol-gel synthesis	500-1300°C	Miscellaneous	Variable	Nano
	Hydrolysis	900°C	Miscellaneous	High	Variable
Hydrothermal		120°C	Spherical or needle shaped	High	Nano or micron
Combination method		-	Miscellaneous	Variable	Most Nano-sized

Although many methods of synthesis have been developed, the preparation of HA with specific characteristics remains challenging to the researchers due to the possibility of the formation of toxic intermediate products during synthesise the HA. Hence, studies on new HA synthesising parameters are still ongoing.

## 2.4 Characterisation of Hydroxyapatite

### 2.4.1 X-ray diffraction

X-ray diffraction (XRD) is easier method to observe the crystalline structure of HA powder. The XRD patterns were obtained using Cu  $K\alpha$  radiation of wavelength ( $\lambda = 1.54056 \text{ \AA}$ ) at 15 mA under a voltage of 30 kV (Khiri *et al.*, 2016). The HA samples were scanned with speed of 1.5°/min in the range of  $2\theta$  angle with scanning range from 10° to 80° and the intensities were recorded. The measurement of samples is used to determine the composition of compound of atomic level. When HA samples are exposed to a beam of x-ray, the angle of diffraction and the intensities of the diffracted beams will measure the composition of the samples or lattice spacing of the crystal. Additionally, the wavelength

remains fixed while angle is scanned as to determine the angle of diffraction of HA sample. Based on this analysis, the Scherer equation is involved as to determine the crystalline size of the sample (Khandelwal and Prakash, 2016).

The advantage of using XRD for HA powder analysis is easy to operate from raw material to data collection (Artioli and Angelini, 2010). It also used cheap instruments available in all laboratories. This is the best method for phase analysis that the x-ray does not absorb too much air. Therefore, this method does not require an evacuated chamber. However, there are some drawbacks in the use of XRD analysis which the x-ray does not interact with the lighter elements. Apart from that, the intensity is ten times less than the electron diffraction (Díaz-Terán *et al.*, 2003).

#### **2.4.2 Fourier transform infrared spectroscopy**

The popular method of infrared spectroscopy is Fourier transform spectroscopy (FTIR). The sample transmits infrared (IR) radiation. The spectrum that occurs is molecular absorption, which produces a molecular fingerprint for the sample. The advantage of using FTIR analysis is that no molecular structures has the same infrared spectrum. Hence, it can use for several types of analysis. It also precisely separates the material which includes some rare and unusual synthetic materials mentioned by Karampelas *et al.* (2011). However, there are some negative effects in the use of FTIR analysis (Levine *et al.*, 1989). The mounted samples may obstruct the IR beam, which can usually be tested only by small samples in this analysis. In addition, several materials can completely absorb IR, which may be impossible to achieve a reliable result.

#### **2.4.3 Vickers hardness tester**

The Vickers hardness test is indicated to measure the mechanical hardness which consisting of diamond indenter, right pyramid shape that has a square base and an angle of  $136^\circ$  between opposite sides and a load between 1 and 100 kgf. Typically, the load is placed in between 10 to 15 seconds. After the load is removed, the two indentation diagonals left in the surface are measured by a microscope (Chandler, 1999).

The advantage of the Vickers hardness test is very precise readings. Thus, it can use one type of indenter to measure the metals and surface process. However, Vickers' machine is more costly compared to Brinell's or Rockwell's, for testing the mechanical hardness of materials with different load.

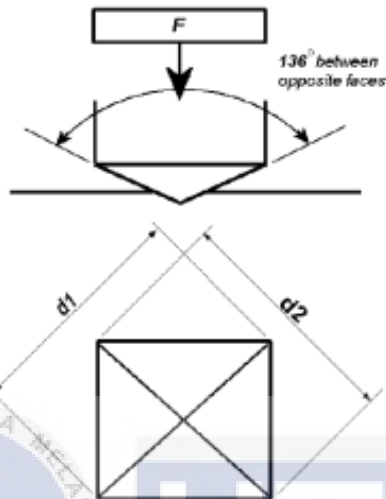


Figure 2.4: Principle of Vickers Hardness Tester (Chandler, 1999).

#### 2.4.4 Scanning electron microscopy

Choudhary and Choudhary (2017) stated that Scanning Electron Microscopy (SEM) is made up of electron microscopes are based on same basic concepts as the light microscopes. A SEM analysis provides surface information by monitoring a sample with an electron beam in a raster pattern. It also produces three-dimensional images of black and white where the image magnification may be up to 10 nm. Deeper vision, high resolution and more accurate image of the surface are given by intensive interactions on the surface of the specimen.

Extensive three-dimensional and topographic images as well as flexible information from different detector modules are part of the benefit of using SEM for analyses. SEM is also easy to use with proper computer technology training with development and related software as to makes the system easy to run. This analysis works quickly which can be done less than five minutes. Moreover, results in improvement enable the development of digital data. However, there are some drawbacks in the use of SEM analysis which is size and cost.

This analysis is very costly and large device that is necessary in an area free of possible interference from electrical magnetic and vibrational effects.

#### 2.4.5 Particle size analyser

Particle size analyser (PSA) is used to obtain data on average particle size, particle size distribution and particle shape as well as to ensure the quality of the samples (Jonasz and Fournier, 2007). Characterization techniques for particle size can detect any deviations from the expected size of particles which then confirm that impurity is exists. There are two technique involve in characterize the particle size which either wet method or dry method (Dhamoon *et al.*, 2018).

The advantage of using PSA analysis is offers flexibility in sample performance. This analysis also fast which took five minutes per sample as well as gives the reliable result. However, there are some drawbacks where this technique have low resolution and not suit for strong absorb materials (Dhamoon *et al.*, 2018).

#### 2.5 Natural Hydroxyapatite

Normally, biological or waste sources such as mammalian bones, aquatic sources, shells and even mineral sources such as limestone can extract the natural HA, Calcium and phosphorus are classified as stoichiometric HA with a Ca/P molar ratio of 1.67 (Szcześ *et al.*, 2017). Generally, this ratio had proved to support bone regeneration (Akram *et al.*, 2014; Wagh, 2016). Nevertheless, Pu'ad *et al.* (2019) indicated the non-stoichiometric contained other elements either the Ca or P elements. Figure 2.5 illustrates the origins and examples of techniques employed by the natural HA for synthesis.

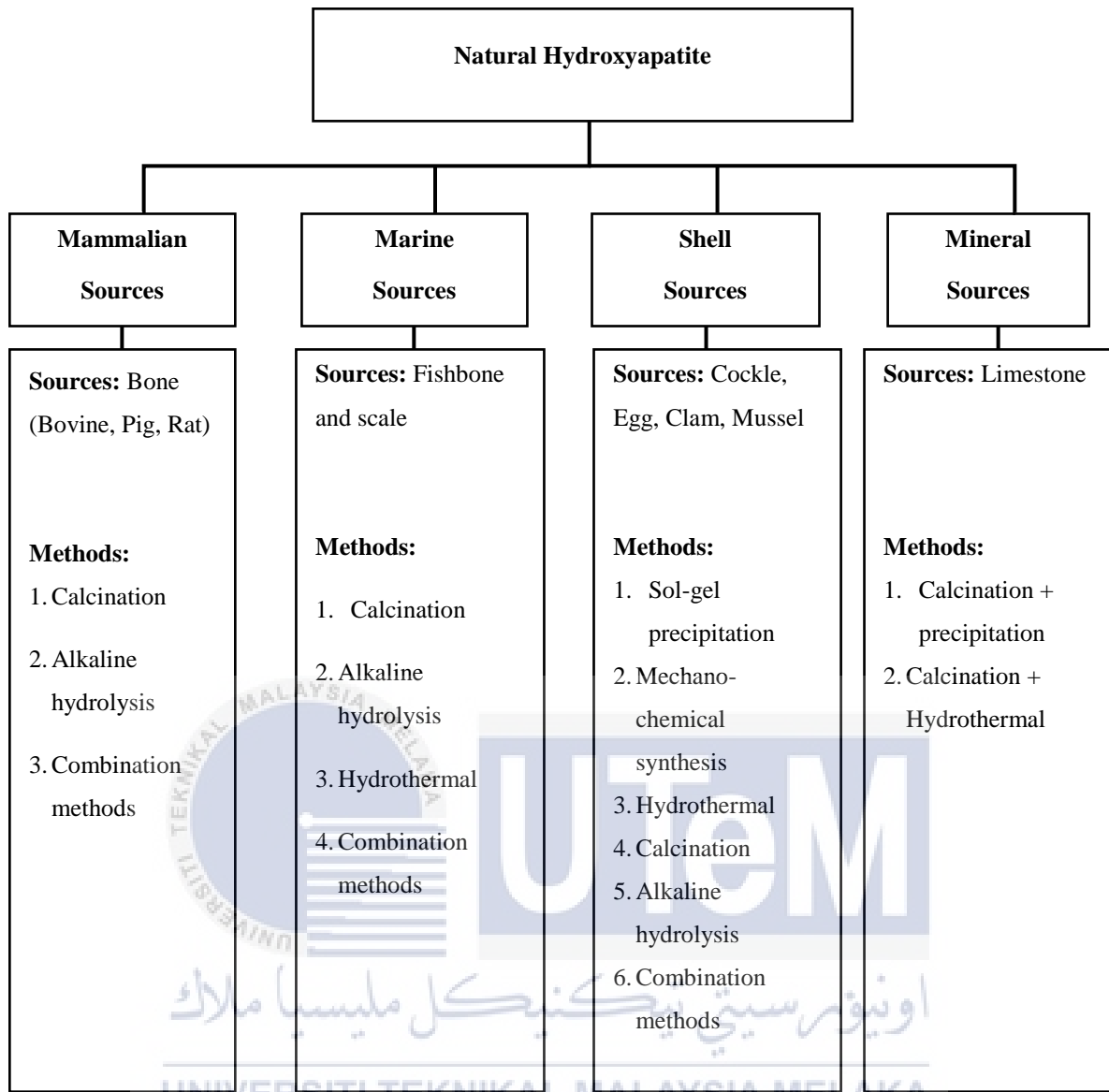


Figure 2.5: Summary of extracting HA from natural sources (Pu'ad *et al.*, 2019)

The use of HA derived from natural sources could be products that are environmentally friendly, safe and economical, since it can be used in large quantities. This work contributes to achieving the goal of raising consciousness about potential ways of generating economic returns from natural waste. Despite being regarded as impurities of the HA system, the foreign matter, as seen in HA from natural sources, is beneficial for bone growth and supports biological functions. Unlike synthetic HA (stoichiometric HA), Ramesh *et al.* (2018) mentioned that normally, carbonate ions are found in natural HA as impurity.  $\text{CO}_3^{2-}$  found in natural HA known to be a major compound for bone replacement as bio-reabsorbing. The characteristics of HA rely heavily on extraction method used. Based on biological apatite, multiple substitutions and deficiencies have been identified in all ion sites. The B-type carbonate HA should be emphasized in all of the compounds where the phosphate ions were replaced with carbonate.

### 2.5.1 Extraction of hydroxyapatite from natural sources

Based on mammalian sources, Pu'ad *et al.* (2019) analysed that many researcher had done research the extraction of HA from bovine (cow) bone compared to other sources such as pig, rat and so on. The cortical section of the femoral bone is typically used as it resembles to the human bone based on morphology and structure (Bluemel *et al.*, 2015). Pu'ad *et al.* (2019) also state that properties of extracted HA, such as Ca/P ratio, size, shape and crystalline phase of CaP, have been discussed as these properties differ from the extraction methods used, for example calcination temperatures and pH value. In general, most literatures report that before the extraction process, bone pre-treatment is usually performed. Before surgery, soil, fat, protein and other components including bone marrow and soft tissue is cleaned and washed. Some literatures have documented the use of boiling water in boiling times of about 8 hours to extract organic components from the bone (Ayatollahi *et al.*, 2015). For bone pre-treatment, generally, Hosseinzadeh *et al.* (2014) said that they used solvents such as acetone and chloroform in boiling and washing process. Another pre-treatment process commonly used is washing the bone to remove the soft tissues using surfactants and alkaline solutions. Before or after the elimination of organic members, the bone was cut into smaller pieces. Most literature suggests that the bone was first cut into smaller pieces before boiling or treated with solvent to remove unwanted components like

bone marrow from the bone. (Hosseinzadeh *et al.*, 2014; Ayatollahi *et al.*, 2015; Sun *et al.*, 2017).

Based on marine sources, the increasing fish consumption in the worldwide has led to a considerable increase in fish waste production, especially in scales and bones. The used of fish scales and bones enables HA to be extracted and solid waste in the fishery industry will decrease (Panda *et al.*, 2014). Ca, P and  $\text{CO}_3^{2-}$  are rich in fishbone, which makes it the main source of HA (Pu'ad *et al.*, 2019). In general, pre-treatment is had been done as to remove unnecessary waste on the scales and bones. Some literature said that scales and bones were boiling after the pre-treatment as this process is one of the standard procedure (Sunil and Jagannatham, 2016; Paul *et al.*, 2017). In addition, The fishbone or scales are also pre-treated by tap water rinsing and then immersed in low concentration for the treatment process which using HCl (0.1–1M HCl) mentioned by Sunil and Jagannatham (2016). Usually, before further treatment, fishbone and scales were cut into pieces. Table 2.4 depicts the summary method used to extract HA from fishbone.

Table 2.4: Summary method used to extract HA from fishbone (Pu'ad *et al.*, 2019).

Source	Method	CaP ratio	Crystalline phase	Particle size	Shape
Fishbone	Calcination (Pal <i>et al.</i> , 2017)	1.62	HA + TCP at 1000°C	5-55 nm	Irregular
	Calcination (Sunil and Jagannatham, 2016)	1.63	HA (1000°C)	64.5- 330 nm	Agglomerate
	Calcination (Ahmad Fara <i>et al.</i> , 2015)	1.76	HA (1000°C)	-	Irregular
	Alkaline heat treatment (Venkatesan <i>et al.</i> , 2015)	-	HA	6- 37 nm	Irregular

Therefore, HA can be transformed into other CaP phases such as  $\beta$ -TCP at high temperatures by using calcination methods. However, the alkaline heat treatment method will produced pure HA phase but with lower crystallinity compared to the calcination method. In general, most of the methods listed may produce nano sized HA with different morphologies. Hence, the limitation in this research which using calcination method is the purity of HA.

## 2.6 Overview of Fish

Tuna fish is known as a value improvement to the increase in fish production in Malaysia. The Malaysian Government has taken initiatives to evolve tuna fishing sectors from coastal areas within the Exclusive Economic Zone (EEZ) and open sea, particularly in the South China Sea. There are over 100 fish species in Malaysian Sea. Tuna species accounted for 5% of the total marine catch in the Malaysian Sea reported by Basir *et al.* (2016). It has been traded which have protein source and it is common eaten by the local community as their local dishes. In fact, Malaysia is located in the western part of the Maritime Continent, Southeast Asia. The Malacca Straits and the South China Sea are the two main areas that contribute the catch of tuna. Oceanic tuna species are found in Malaysian Sea and the main species are Skipjack Tuna (*Katsuwonus pelamis*), Yellowfin Tuna (*Thunnus albacares*), Bigeye Tuna (*Thunnus obesus*) and Albacore Tuna (*Thunnus alalunga*) while the Neritic Tuna found are Longtail Tuna, Frigate Tuna, Bullet Tuna and Kawakawa Tuna.

### 2.6.1 Production of Tuna fish in Malaysia

25 years of statistics on production of Tuna fish were observed from the source of Department of Fisheries (DOF) Statistic Report (1990 until 2015) stated by Basir *et al.* (2016). The data showed unstable production of two species Tuna fish throughout the years. Figure 2.6 reveals the highest production of Longtail Species occurred in 2007 and the lowest production in 1994 based on 25 years statistics. However, the highest production of Kawakawa species occurred in 2012 and the lowest production in 1994.



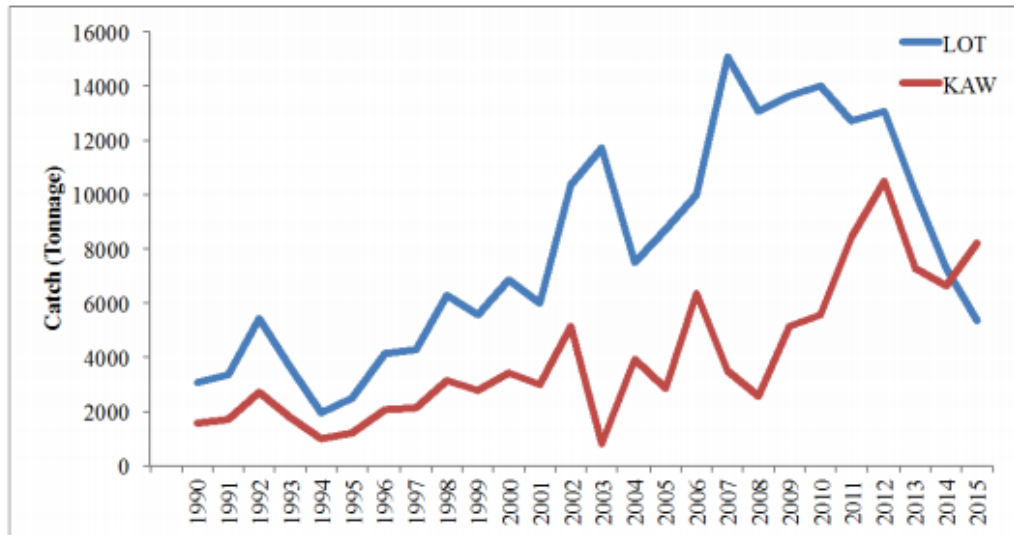


Figure 2.6: The production of Tuna Fish (Kawakawa and Longtail) in Malaysia (1990-2015) source from Department of Fisheries (DOF) statistics report

Malaysia's tuna production is expected to increase to 80% by 2020 till 2030. It has been noted that the majority of tuna production is exported to other country specifically in Europe and Japan. Hence, only a small percentage of the catch was consumed by Malaysians (Department of Fisheries Malaysia, 2014). Skipjack Tuna is known as one of the most widely recognised fish commodities in the Malaysian Sea. It is focusing to increase the value of commercial fishery in Malaysia. However, they are sensitive to the environmental conditions as they are capable of large-scale relocation to identify the good environmental condition that satisfies physiological needs of *Skipjack Tuna* fish (Boniface *et al.*, 2018). Based on the previous study by Zainuddin *et al.* (2017) mentioned that the migration of *Skipjack Tuna* fish are strongly influenced by ambient temperature and dissolved oxygen concentration. The potential habitat of this species is in a warm surface layer of the tropical oceans specifically at the South China Sea. South China Sea is the best characteristics of tropical oceans as because the sea surface temperature (SST) is relatively constant. Tan *et al.* (2002) mentioned that SST of the South China Sea is the range between 28°C to 32°C specifically in May or June (warmer months), while the range of SST between 25.2°C to 28.8°C specifically in December or January known as the cooler months.

## 2.6.2 Synthesis of fishbone-based hydroxyapatite

The use of waste material as a basic material has attracted a great deal of attention to support the sustainability programme. The development of a HA-synthesis based on waste materials is one of the application that support the sustainability program. Eggshells (Khandelwal and Prakash, 2016), sea shells (Santhosh and Prabu, 2013) and cockle shells (Razali *et al.*, 2016) are some of the waste that can be used for synthesis HA. The waste material has been chosen because it has high calcium levels and thus allows for the production of calcium phosphate with the addition of phosphates at certain levels. One of Malaysia's rich waste is fishbone. This is because fish is the primary protein source in Malaysia. The fishbone is rich in calcium content, phosphate, and carbonate which make it a great source for extraction of HA.

Calcination process is a standard procedure to synthesis HA from fishbone which is known as a process involving transferring thermal energy from the specimen, transfer thermal energy from external surfaces to the internal samples interface, the absorption of heat and the thermal decomposition of the interface surface layer, the dissemination by a pore of CaO to formed CO<sub>2</sub> and the diffusion of CO<sub>2</sub> at the atmosphere. The reaction continues if the partial pressure of CO<sub>2</sub> is less than the equilibrium value. Various researchers have reached a strong consensus on the equilibrium of calcite decomposition. Some research stated by Cahyanto *et al.* (2017) that fishbones are transformed into HA by the thermal decomposition method. However, in the final product, some carbonate functional group (CO<sub>3</sub><sup>2-</sup>) were found in the hydroxyapatite phase. Previous studies by Venkatesan *et al.* (2015) mentioned they were using a simple calcination technique to produce HA from raw fishbones also agreed that final product was given a mixture of HA, TCP and β-TCP. Zainol *et al.* (2019) also mentioned that the preparation of synthetic HA from raw fishbone can be done by using an alkaline method which is synthesized by using a long term alkaline process to support HA as a precursor for calcium.

## 2.6.3 Characterisation of fishbone

### 2.6.3.1 Physical composition of fishbone

*Skipjack tuna* has a dark blue colour with a complicated striped pattern. The length of *Skipjack tuna* depends on its age, location and sex. The maximum size reported for Pacific *Skipjack tuna* is approximately 99 cm and the maximum weight is approximately 19 kg. Based on figure 2.7 below shows the measurement of fish size (Pornchaloempong *et al.*, 2012). The size of the fish is determined by the measurement of length, height and width.

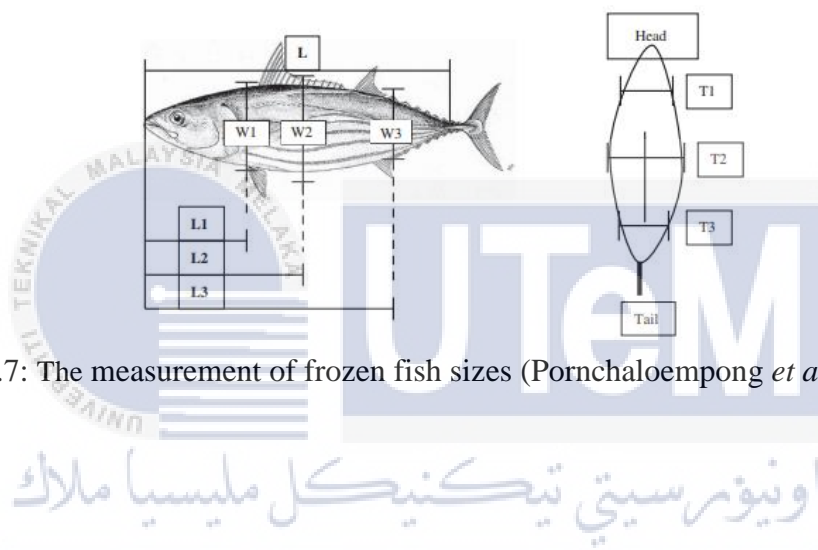


Figure 2.7: The measurement of frozen fish sizes (Pornchaloempong *et al.*, 2012)

### 2.6.3.2 Chemical composition of fishbone

Yoon *et al.* (2018) stated that *Skipjack tuna* fish containing 71.76% by weight of moisture, 25.29% of protein, 0.87% carbohydrates and 0.60% of fat. They also revealed that fishbone consists of 30 kinds of fatty acid. *Skipjack tuna* meat yield (58%) was greater than the bone (25%) and offal (17%). This is supported by the characteristics of tuna that have a dense and compact meat texture. Meat is part of Skipjack's body, which is very commonly used. The results of this study show that *Skipjack tuna* contained some amino acids.

Table 2.5: The Amino acid contains in *Skipjack tuna*

Amino acids	<i>Skipjack tuna</i> bone (a) (residues/ 100 residues)	Fresh <i>Skipjack tuna</i> (b) (g/100g)
Aspartic acid	46	7.35 ±0.11
Threonine	30	3.30 ±0.05
Serine	37	2.69 ±0.04
Glutamic acid	77	11.22 ±0.14
Glycine	337	4.83 ±0.20
Alanine	125	5.04 ±0.09
Methionine	15	2.16 ±0.04
Leucine	27	5.89 ±0.05
Tyrosine	7	2.54 ±0.04

Source: a) (Ding et al., 2019); b) (Suseno et al., 2015)



## **CHAPTER 3**

### **METHODOLOGY**

#### **3.1 Overview**

This chapter explain the methodology to synthesise HA from fishbone. The process starts from the cleaning of the fishbone, calcination process, and preparation of HA powder. Then, the synthesized HA powder will be characterized and analyse to discuss the properties. The flow chart in Figure 3.1 represents the experimental procedure involved in this study. The detailed processes of the preparation and characterization of synthetic HA from fishbone explained in this chapter.

#### **3.2 Materials and Equipment**

The material used in this research were fishbone that obtained from a fish market at Mersing, Johor, distilled water from Fakulti Kejuruteraan Pembuatan, Universiti Teknikal Malaysia Melaka, and commercial HA produced from REKAGRAF<sup>TM</sup> Laboratory SMMRE, Engineering campus Universiti Sains Malaysia, Penang. While the equipment will use in this study are electrical furnace, pestle and mortar as well as manual hydraulic press machine.

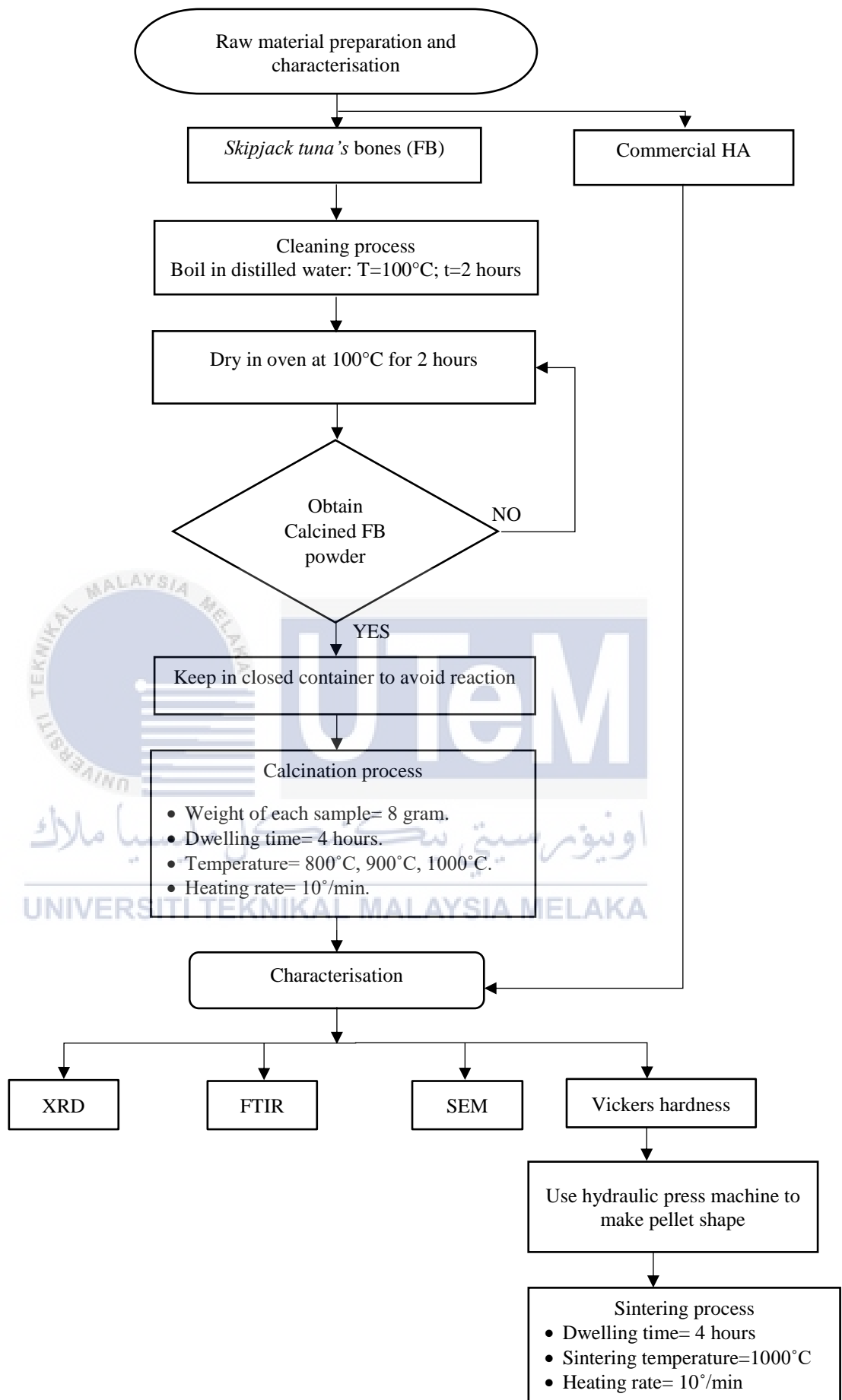


Figure 3.1: Schematic flow process chart of preparation and characterisation of HA from fishbone

### 3.3 Experimental






The experimental procedure setup is divided into three stages: the preparation of fishbone powder, the preparation of synthetic HA pellet as well as the characterisation of synthetic HA.

#### 3.3.1 Preparation of fishbone powder

The preparation of HA from FB was adopted from techniques that has previously been described by Pal *et al.* (2017) and Sunil and Jagannatham (2016). The collected FB waste were washed and cleaned with water to remove flesh and blood to ensure it is clean from contamination. Then, FB filler was dried in the oven for one hour. Subsequently, dried FB was store in a desiccator to avoid any reaction with CO<sub>2</sub> and reduced the adsorption of humidity. Then, the samples were characterised by using X-ray diffraction, XRD (Model: Panalytical X'pert Pro) to confirm the presence of elements in samples.

The samples of dried FB were calcined for four hours using electrical furnace in three different temperature; 800°C, 900°C and 1000°C that labelled as A800, B900 and C1000 with a heating rate of 10°/min. The calcined samples were cooled in the furnace itself at room temperature. Calcination process is known as the best method to produce HA as it is easy and low cost method. The calcined FB were crushed by using pestle and mortar. Then, the calcined FB powder was store in a desiccator to avoid any reaction with CO<sub>2</sub> and reduced the adsorption of humidity. The calcined FB powder were characterised by using XRD, FTIR, SEM and Vickers Hardness. Table 3.1 below indicates the process of the preparation of FB powder. The commercial HA powder that labelled as C-HA was obtained as a reference for the purpose of comparison with synthetic HA powder from FB at different calcination temperature.

Table 3.1: The preparation of fishbone powder

Clean the FB	De-protein FB	Dried FB	Calcined FB	FB powder
				

### 3.3.2 Preparation of synthetic HA pellet

Two gram of calcined FB powder of three different temperature manually press by using hydraulic press machine with compaction pressure of 5 tons for two minutes to form HA powder into green pellet shape of dimension of 10 mm x 7 mm. The pellet samples were sintered in the electric furnace at 1000°C for four hours based on research by Obada *et al.* (2020) and cooled in the furnace itself at room temperature. The synthetic HA pellet were then polish as to obtain smooth surface for better result.

### 3.3.3 Characterisation of synthetic HA from fishbone

#### 3.3.3.1 X-ray diffraction analysis (XRD)

The structural properties of the samples were analysed using an X-ray diffractometer (Model: Panalytical X'pert Pro). The analysis run at 40 kV and 30 mA with Cu K $\alpha$  alpha radiation, ( $\lambda = 1.54056 \text{ \AA}$ ) which will give good resolution in the pattern of samples. The samples were recorded at peak position of  $2\theta$  angle with scanning range from 10° to 80°. Each scan was set the step size is 0.02 and scan speed 2°/min. The Scherer formula shows in equation [2] is used to determine the crystallite size of the particles in the HA powders from XRD pattern. The broadening of the diffraction peaks is related to the crystallite size either to be equal or smaller to the grain size.

$$D = \frac{K\lambda}{(\beta \cos \theta)} \quad [2]$$



D is stated as the crystallite size,  $\lambda$  is the x-ray wavelength of Cu K $\alpha$  radiation with value of 0.154056 nm, while K is crystallite shape factor. Basically, 0.9 is a good approximation of crystallite shape factor. The full width at half maximum (FWHM) of compound line is known as  $\beta$  and the peak position of  $2\theta$  is denoted by  $\theta$  (Khandelwal and Prakash, 2016).

### 3.3.3.2 Fourier-transform infrared spectroscopy (FTIR)

Fourier-transform infrared spectroscopy (FTIR) analysis was conducted on the HA samples using Jasco FT/IR-6100 series. The FTIR spectra analysis were recorded at a frequency between 400 to 4000  $\text{cm}^{-1}$  (Khiri *et al.*, 2016). The FTIR spectroscopy was equipped with an interferometer used to detect HA powder by producing an optical signal with all the infrared radiation frequencies embedded in it. From the FTIR spectra, the molecular bond structure of the HA samples such as OH $^{-}$ , PO $_4^{3-}$  and CO $_3^{2-}$  was identified and characterised. The existence of the bands corresponding to the HA functional group confirmed the formation of HA structure. The characterisation of sample using FTIR method may be in powder, pellet or bone shape.

### 3.3.3.3 Vickers hardness study

The hardness of the synthetic HA pellet was observed and identified by using a Vickers micro hardness tester (Model: MicroWiZhard) which using pyramidal diamond indenter. The Vickers micro hardness is used to observe and identify the mechanical hardness of the HA. All the sintered pellet sample must polished before do test and the measurement are fixed 300 gram of load in 15 second of dwelling time by taken three indentations value as defined clearly by Khiri *et al.* (2019). There are many reasons for conducting tests under different circumstances. For the reason that it produces a large impression, a high load is selected. Hence, it is easy to measure the indentation diagonal. However, an oversize impression is caused by a high load applied to a soft surface, where the diagonals are longer than the micrometre scale fitted to the tester's eyepiece. Therefore, a small load must be applied in this study for a comparison between the baseline surface and the eroded surface for the same indentation load.

### 3.3.3.4 Scanning electron microscopy (SEM)

The morphology and microstructure of the samples were analysed and studied using the Scanning Electron Microscope (SEM) (Model: EVO50 Carl Zeiss SMT). The purpose of the SEM analysis is to identify an unknown element or compound that may cause interaction between materials. High-resolution SEM analysis imaging will support the size and morphology of particles that can identify the properties of HA powders. The samples were dispersed by using ultrasonic bath in an ultrasonic bath (Model: Power Sonic410) for 15 minutes. Then, the samples were placed on top of the stub which then prepared by gold sputtering the surface of the samples using a low deposition rate. Each gold sputtered sample was viewed at 1,000X and 5,000X and 10,000X.



## CHAPTER 4

### RESULT AND DISCUSSION

This chapter explain the analysis of synthesis and characterisation HA from fishbone from the methodology. This chapter consists of two sections which describes the general observation of raw fishbone and the characterisation synthetic HA analysis from fishbone by compare with commercial HA as a guideline for this study.

#### 4.1 Observation of Raw Fishbone

##### 4.1.1 General overview

The dried *Skipjack tuna* bone was light yellow in colour, which points toward the presence of collagen and other organic materials. The yellow colour disappeared when the raw fishbone (FB) was subjected to the calcination method, as shown in Figure 4.1, signifying the proper removal of collagen and other organic materials. Table 4.1 represents the result of fishbone weight after undergo the calcination process for the production of synthetic HA powder. The selected calcination temperature are 800, 900 and 1000°C which labelled as A800, B900 and C1000. Based on the research by Sunil and Jagannatham (2016), the formation of stable pure HA from fishbone was reported to be at 1000°C. It is different from Mustafa *et al.* (2015) where the formation of pure HA is occurs at 900°C. While Suguna (2019) states that the formation of pure HA from fishbone is between 800 and 1000°C. From this observation, the isolation yield of samples A800, B900 and C1000 is equal to 74.65%, 66.64% and 66.31% respectively.

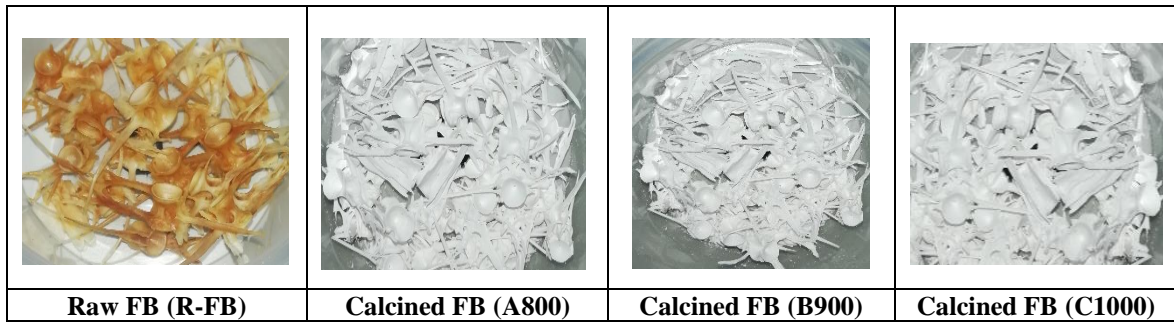


Figure 4.1: General observation of raw fishbone (R-FB) and calcined fishbone at calcined temperatures: 800°C (A800), 900°C (B900) and 1000°C (C1000)

Table 4.1: The calcination data of synthetic HA powders at calcined temperatures: 800°C (A800), 900°C (B900), 1000°C (C1000) and commercial HA (C-HA)

Sample	Calcination Temperature (°C)	Initial Weight (gram)	After Calcined Weight (gram)	Residue (%)	Colour Appearance
R-FB	-	-	-	-	Light yellow
A800	800	12.07	9.01	74.65	White
B900	900	12.05	8.03	66.64	White
C1000	1000	12.08	8.01	66.31	White

#### 4.1.2 X-ray diffraction analysis (XRD)

Based on XRD spectrum, a broad single peak was found in raw bone corresponds at 32.06° known as amorphous phase. It is due to the presence of the fibrous collagen which disperses the X-ray radiations as depict in figure 4.2. This data is parallel to the findings made by Venkatesan *et al.* (2017) that a broad single peak was observed in the XRD spectrum of raw fishbone at 32.7°, confirming that the HA is amorphous. However, Chalisserry *et al.* (2018) observed that a broad single peak was found lies at 20° due to the presence of collagen in the fishbone. Hence, it is conclude that the broad single peak in raw FB was found in the range between 20 to 35° detected at 2θ angle.

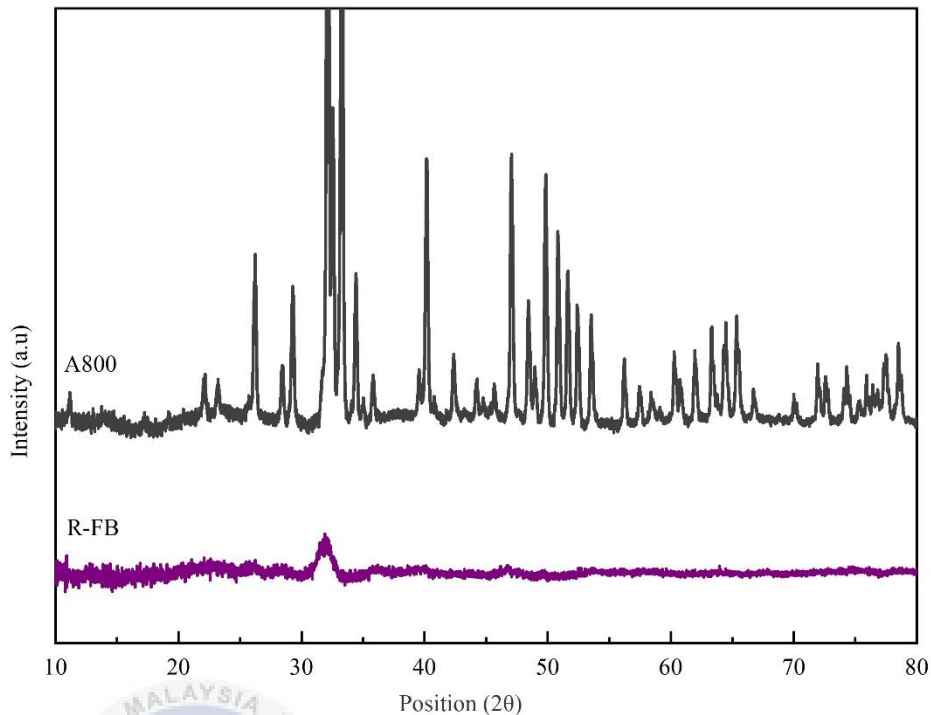


Figure 4.2: XRD pattern analysis of sample raw fishbone (R-FB) compared with sample calcined powder at 800°C (A800)

#### 4.1.3 Fourier-transform infrared spectroscopy (FTIR)

The characteristic R-FB bands were 555.4, 593, 1023, 1447, 1531, 1635, 2853, 2925 and 3282  $\text{cm}^{-1}$ , as tabulated in table 4.2, respectively. The stretching frequencies of raw fishbone (R-FB) are broader than one of the sample from calcined FB powder (A800).

Based on figure 4.3, the variable band at 3282  $\text{cm}^{-1}$  corresponds to O-H stretching due to presents of water in sample. The intense peak at 2925  $\text{cm}^{-1}$  and 2853  $\text{cm}^{-1}$  indicates to the C-H deformation of alkane compounds. The alkanes protect the fish from the loss of water in the bone and prevent the leaching of important minerals. Amide I is known as the most intense protein absorption band. It is generally influenced by the stretching vibrations of the C=O and C-N groups where it was found in the region of 1635  $\text{cm}^{-1}$ . Amide II is found in the 1531  $\text{cm}^{-1}$  region and is more complex than Amide I. Amide II is typically extracted from the bending of the N-H plane, the C-N group and the C-C stretching vibrations. Medium bonds in the 1447  $\text{cm}^{-1}$  region can be described as C-H bond alkanes found in raw fishbone. C-O bond in alcohols with a frequency of 1023  $\text{cm}^{-1}$  was present in the R-FB

sample. Carboxylic acids are very important in the formation of fats in the body of fish that act as strong antibacterial agents.

Table 4.2: FTIR peak value of sample raw fishbone (R-FB)

Wavenumber (cm <sup>-1</sup> )	Bond	Functional Group Assignment	Type Vibration	Intensity	Frequency group (cm <sup>-1</sup> )
3282	O-H	Hydrogen bonded Alcohols, phenols	Stretch	Variable	3200-3400
2925, 2853	C-H	Alkanes	Asymmetric Stretch	Strong	2850-2970
1739	C=O	Aldehydes, saturated aliphatic	Stretch	Strong	1720-1740
1635	Amide I	C=O stretching vibration, Amide I	Stretch	Medium	1600-1800
1531	Amide II	N-H bending vibration and from the C-N stretching vibration	Stretch	Medium	1470-1570
1447	C-H	Alkanes	Deformation	Medium	1445-1485
1023	C-O	Primary alcohol	Stretch	Strong	1000-1075
593, 555.4	C-I	Aliphatic iodo compounds, C-I stretch	Stretch	Strong	500-600

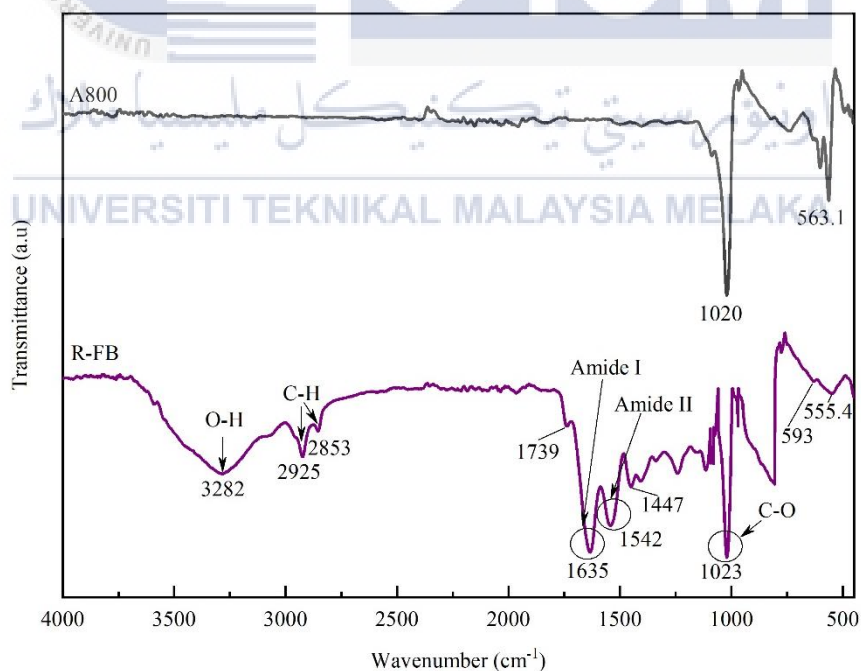





Figure 4.3: FTIR spectrum analysis of sample raw fishbone (R-FB) compared with sample calcined powder at 800°C (A800)

#### 4.1.4 Synthetic HA pellet analysis

When the FB powder has undergone the process of pressing the mould to produce the shape of the pellet, it will be sintered. Table 4.3 shows the sample appearances after undergo the sintering process at temperature 1000°C that provide compact cylinder shape. Visual inspection was carried out to the sample. The surface colour of the pellet sample C1000 more white when compared with sample A800 and B900. However, after the green pellet were subjected to the sintering process, the colour of all pellet sample turn to white in colour and no crack was observed in the sample.

The porosity of the sample is decrease when subjected the green pellet to the best sintering temperature which can be explained by the densification of the sample revealing the removal of porosity at high sintering temperatures. It is agreed by Mouiya *et al.* (2019) where the apparent porosity of their sample is decrease when the sintering temperature is increase. Hence, the sintering temperature is able to promote the high densification without affecting the shape of sintered pellet.

Table 4.3: Physical appearance of sintered pellet at sintering temperature 1000°C

Sample	A800	B900	C1000
Green pellet before sintering process			
Justification	Crack at the edge	No crack	No crack



## 4.2 Characterisation of Synthetic HA Analysis from Fishbone

### 4.2.1 X-ray diffraction analysis (XRD)

XRD analysis has been developed as to ensure the heat treatment process is not affected the chemical structure of HA present in fishbone. The HA phase is characterised by the main intensity at a  $2\theta$  value. The XRD patterns of the samples show major HA-corresponding reflections and fewer CaP-reflections as shown in Figure 4.4. After the calcination process at 800, 900 and 1000°C for four hours, the intensity of the HA phases in the samples was clearly defined as shown by the increasing sharp and narrow peaks in the XRD pattern signalling the effect of sintering by the production of pure HA, which is in good correlation with the standard values for commercial HA as well as the standard HA (Joint Committee on Powder Diffraction Standards, Card no. 00-001-1088). Based on the result, the highest intensity peak with 100% intensity detected at  $2\theta$  angle of 32.15° for sample A800, 32.03° for sample B900, 31.96° for sample C1000, while the C-HA is at 32.08°.

As the temperature is increase, the peaks of intensity also increase. Therefore, the HA sample is more pure and stable. In this study, CaP and HA were detected from sample A800. However, when the temperature of heat treatment process increases, the CaP reflection in XRD pattern is decreases. In addition, the heat treatment process of fishbone releases collagen and proteins that are bound to fishbone. The CaP group that can be found in the samples are  $\beta$ -tricalcium phosphate ( $\beta$ -TCP),  $\alpha$ -tricalcium phosphate ( $\alpha$ -TCP), Calcium pyrophosphate (CPP) and Calcium metaphosphate (CMP). Pal *et al.* (2017) mentioned that the  $\beta$ -TCP phase was formed in calcined fishbone powder due to the low Ca/P atomic ratio where from their research found a fewer reflection of  $\beta$ -TCP phase was formed at calcination temperature 800, 1000 and 1200°C. Based on the result, the calcination temperature changed the contents of HA and CaP reflection in XRD pattern. Hence, it is confirms the predominance of HA and CaP was formed in the samples.



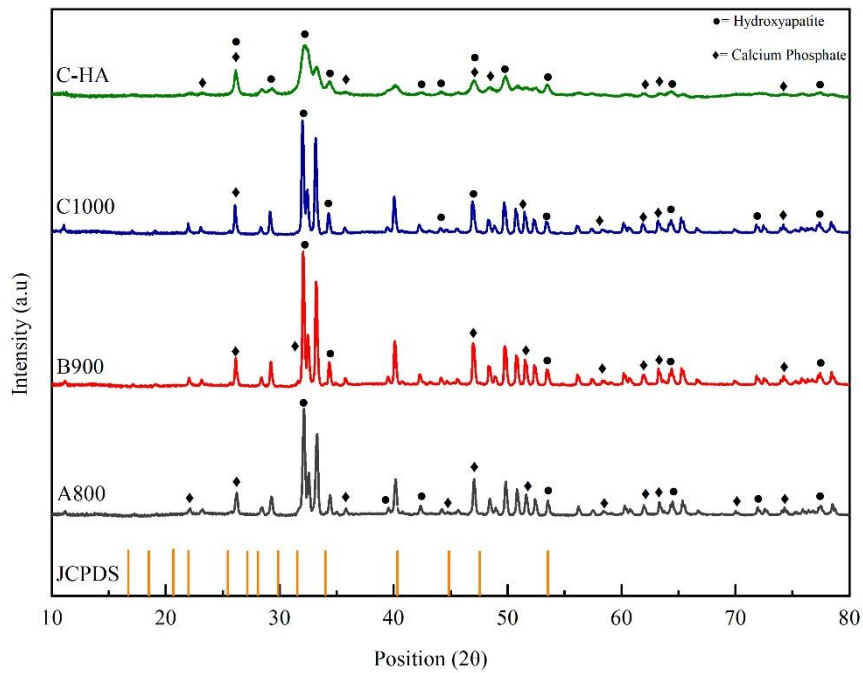


Figure 4.4: XRD pattern analysis of synthetic HA powders at calcined temperatures: 800°C (A800), 900°C (B900), 1000°C (C1000) and commercial HA (C-HA)

The crystallite size of the sample is calculated by using Scherrer equation and the results are tabulated in Table 4.4. The crystal size in the obtained powders of A800 is 44.91 nm, while it increases to 46.10 nm for sample B900 and 63.17 nm at sample C1000. This result is in accordance with the sharpness of the XRD peaks and high crystallite size when the temperature is increased from 800 to 1000°C. According to Hariani *et al.* (2020), when the particle sizes are in nanoscale size which is less than 100 nm is classified as nano HA.

Table 4.4: The crystallite size of powder for synthetic HA powders at calcined temperatures: 800°C (A800), 900°C (B900), 1000°C (C1000) and commercial HA (C-HA)

Sample	Calcination Temperature (°C)	Peak Position (2θ: 32°, 53°)	FWHM	Intensity (%)	Average Crystallite size, D (nm)
A800	800	32.15	0.25	100	44.91
		53.51	0.13	13.64	
B900	900	32.03	0.18	100	46.10
		53.41	0.19	11.72	
C1000	1000	31.96	0.17	100	63.17
		53.37	0.10	10.36	
C-HA	-	32.08	0.27	100	34.13
		53.45	0.23	22.14	

#### 4.2.2 Fourier-transform infrared spectroscopy (FTIR)

After heat treatment process, the O-H bond is absent due to the loss of water in this network. Therefore, the FTIR spectra of the samples; calcined powder at 800, 900 and 1000°C completely change the shape of frequency as shown in figure 4.5. In particular, FTIR analysis confirms that pure HA was obtained by referring to the commercial HA (C-HA). All HA typical peaks are visible. HA is the main mineral component of the biological bone absorption because of the vibrational mode of the phosphate ( $\text{PO}_4^{3-}$ ), carbonate ( $\text{CO}_3^{2-}$ ) and hydroxyl ( $\text{OH}^-$ ) groups. This experimental result is compared with previous research by Shi *et al.* (2018) and Kashkarov *et al.* (2011). Generally, there are four vibrational modes present for phosphate ions,  $\nu_1$ ,  $\nu_2$ ,  $\nu_3$  and  $\nu_4$  where FTIR spectrum can observe all the vibrational modes. Based on table 4.4, the  $\text{PO}_4^{3-}$  ions group has resulted in three internal modes which are  $\nu_1$ ,  $\nu_3$  and  $\nu_4$ . The  $\nu_3$  band has two different results. The asymmetric stretching mode of the  $\nu_3$  vibration is characterised by a strong and complex band at a frequency of 1091 and 1042  $\text{cm}^{-1}$ . The bending vibration of  $\nu_4$  are assigned at two sites at frequency of 560-600  $\text{cm}^{-1}$  occur at all samples as shown in figure 4.5. This splitting of the  $\nu_4$  vibrational band indicates the low site symmetry of molecules, as two bands confirm the presence of more than one site for the  $\text{PO}_4^{3-}$  group. The bending vibration of  $\nu_1$  are assigned at frequency of 961  $\text{cm}^{-1}$ .

Biological apatite contains 4 to 8% of  $\text{CO}_3^{2-}$  by weight (Vallet-Regí and Navarrete, 2016; Siddiqi and Azhar, 2020), which is why it was considered useful to include carbonate-substituted apatite in this study. However, biological apatite might lose carbonate groups by sintering it in temperature of 850°C for two hours who was observed by Liu *et al.* (2013). Based on this study, the  $\text{CO}_3^{2-}$  group resulted in one internal mode as shown in table 4.5. Theoretically,  $\text{CO}_3^{2-}$  have four vibrational modes. However, in FTIR spectrum, it can observe  $\nu_2$  and  $\nu_3$  vibrational modes. At a frequency of 1410-1470  $\text{cm}^{-1}$  is described as  $\nu_3$  vibration of a high-energy C-O region which found in sample C-HA lies at frequency 1429  $\text{cm}^{-1}$ , while no  $\nu_2$  vibration of a low-energy C-O region was found in the samples. It is because the  $\nu_2$  carbonate vibration depends on the  $\text{CO}_3^{2-}$  substitutes for the  $\text{OH}^-$  ion and the  $\text{PO}_4^{3-}$  ion in the HA lattice. Besides, the presence of  $\nu_2$  and  $\nu_3$  vibrational modes of carbonates in previous research may contribute to the decrease of  $\text{OH}^-$  in the spectrum. The substitution of  $\text{CO}_3^{2-}$  is critically relevant for the bone mineral phase and has been shown to have osteointegration, biocompatibility and earlier bio-resorption (Siddiqi and Azhar, 2020).

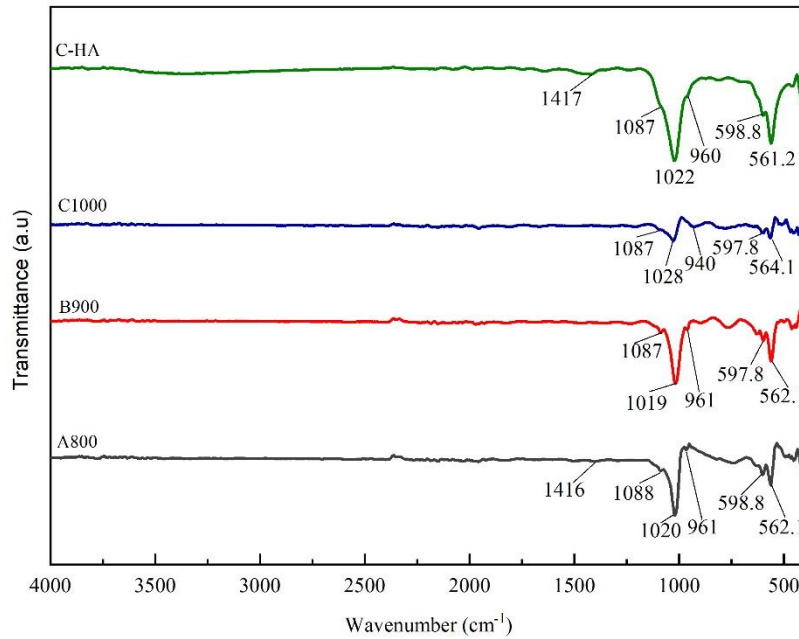


Figure 4.5: FTIR spectrum analysis of synthetic HA powders at calcined temperatures: 800°C (A800), 900°C (B900), 1000°C (C1000) and commercial HA (C-HA)

Table 4.5: FTIR spectrum observation band positions of synthetic HA powders at calcined temperatures: 800°C (A800), 900°C (B900), 1000°C (C1000) and commercial HA (C-HA)

Functional group assignment	Frequency group (cm <sup>-1</sup> ) (a)	Frequency group (cm <sup>-1</sup> ) (b)	Experimental frequency (cm <sup>-1</sup> )			
			A800	B900	C1000	C-HA
Carbonate $\nu_3$ (medium)	-	1429	1416	-	-	1417
Phosphate $\nu_3$ bending (variable stretch)	1090	1090	1088	1087	1087	1087
Bending $\nu_3$ bending (variable stretch)	1040	1050	1020	1019	1028	1022
Phosphate $\nu_1$ (medium stretch)	960	961	961	961	940	960
Phosphate $\nu_4$ (bending)	603	607	598.8	597.8	597.8	598.8
	565	-	562.1	562.1	564.1	561.2

Source for the frequency group: a) (Shi et al., 2018); b) (Kashkarov et al., 2011)

### 4.2.3 Vickers hardness study

The Vickers hardness of the synthetic HA pellet samples with different calcination temperatures (800, 900 and 1000°C) sintered at 1000°C was measured and recorded in table 4.6. In this characterisation, the raw fishbone (R-FB) was not obtained due to the difficulty of forming it in the pellet, as there is no suitable machine for blending it and converting the material into powder before forming it into a pellet. This study shows the hardness of the sample increased rapidly from 0.55 GPa to 0.64 GPa recorded error  $\pm 0.05$  with 5 tons compaction pressure, as shown in figure 4.6. However, it is contrary to the discovery made by Obada *et al.* (2020) where they found that the hardness of synthetic HA increased rapidly from 0.69 GPa to 1.09 GPa with 500 pa compaction pressure sintered at 900, 1000 and 1100°C. From the results, it also can be seen that the calcined powder at 1000°C shows the highest hardness compared to the other temperatures (800 and 900°C).

The increase of hardness is related to the high phase stability of the HA by bonding between the grains in the sintered samples. The increase in the hardness measurement for the synthetic HA sample obtained is in good agreement with previous study. The samples tend to be more compact in this phase and eliminate the porosity. Butkovic *et al.* (2012) indicated that the high sintering temperature can cause the atomic diffusion. Thus, the crystal boundaries in the sample were migrating more rapidly and form a denser material. As a consequences, the hardness of the HA becomes tougher and harder. Theoretically, the Vickers micro hardness values of synthetic HA are larger than the human femoral cortical bone (Obada *et al.*, 2020). Based on previous study by Mirzaali *et al.* (2016) revealed that the hardness of cortical bones of humans aged between 46 and 99 years was in the range of 0.3-0.6 GPa while the range of hardness obtained in this study was between 0.55-0.64 GPa. Therefore, the hardness values of the synthetic HA are in the range of actual human femoral cortical bone.

Table 4.6: The Vickers hardness of synthetic HA powders at calcined temperatures: 800°C (A800), 900°C (B900) and 1000°C (C1000)

Samples	Temperature (°C)	Vickers Hardness value (Hv)			Average Hardness (Hv)	Average Hardness (GPa)
		1	2	3		
A800	800	55.7	55.7	55.4	55.6	0.55
B900	900	57.2	61.2	61.9	60.1	0.59
C1000	1000	65.3	65.3	64.6	65.1	0.64

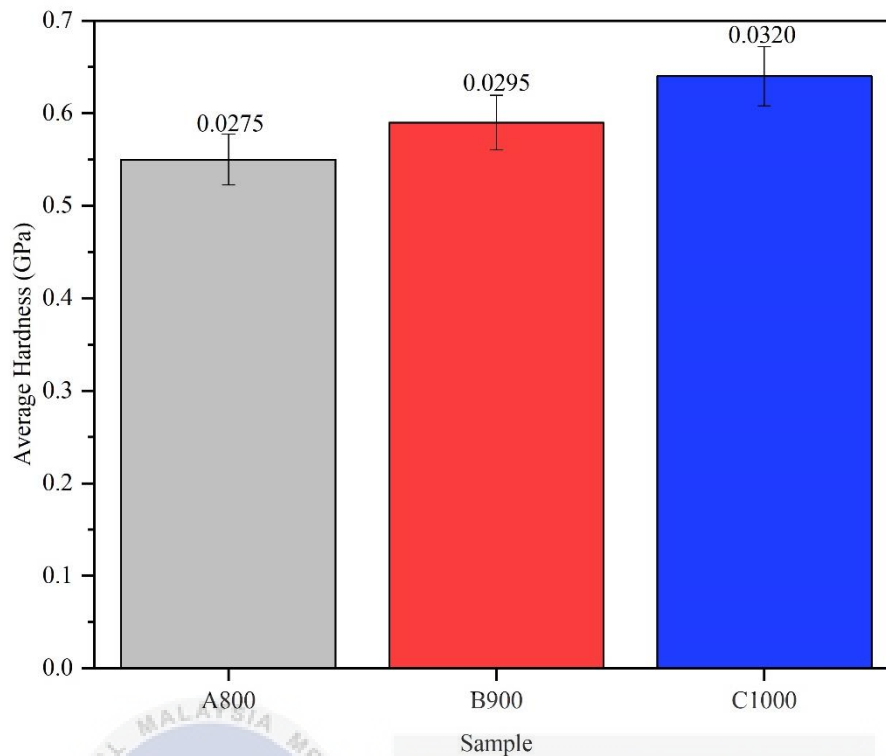


Figure 4.6: Hardness with 5 tons compaction pressure analysis of synthetic HA powders at calcined temperatures: 800°C (A800), 900°C (B900) and 1000°C (C1000)

#### 4.2.3 Scanning electron microscopy (SEM)

Figure 4.7 shows the SEM images of the calcined HA from 800 to 1000°C as well as commercial HA. The stage of evolution of the microstructure of calcined HA samples, which are grouped into highly agglomerated nanoparticle plates can be observed. The agglomerate shape of the particles with a similar structure for every sample was observed at a temperature of 800, 900 and 1000°C. It is agreed by previous research of Sunil and Jagannatham (2016), where the morphology of the crystals for HA is agglomerate in shape composed of tiny crystals. Figure 4.7(a) shows that calcined powders at 800°C had the size of the crystals between 30 to 50 nm, whereas crystal agglomeration occurs in the calcination method. The formation of nanoparticles in the derived HA by heat treatment at 900°C was clearly shown in Figure 4.7(b) between 0.5 to 2 μm. At a temperature of 1000°C, the HA morphology became granular in shape and the irregular HA grain was observed as shown in Figure 4.7(c). Besides, the commercial HA presents agglomeration of small grains that form a grain of higher dimension clearly shown in figure 4.7(d).



All the calcined powders were argued to have different particle sizes. The particle size was projected to increase concerning the temperature. The necking between the particles becomes more prominent in this temperature due to high calcination temperature. The dense grain has become significant at 1000°C and the shape of the denser packing grain has been observed. Therefore, calcined samples at 1000°C were observed to have larger particles than calcined samples at 800°C.

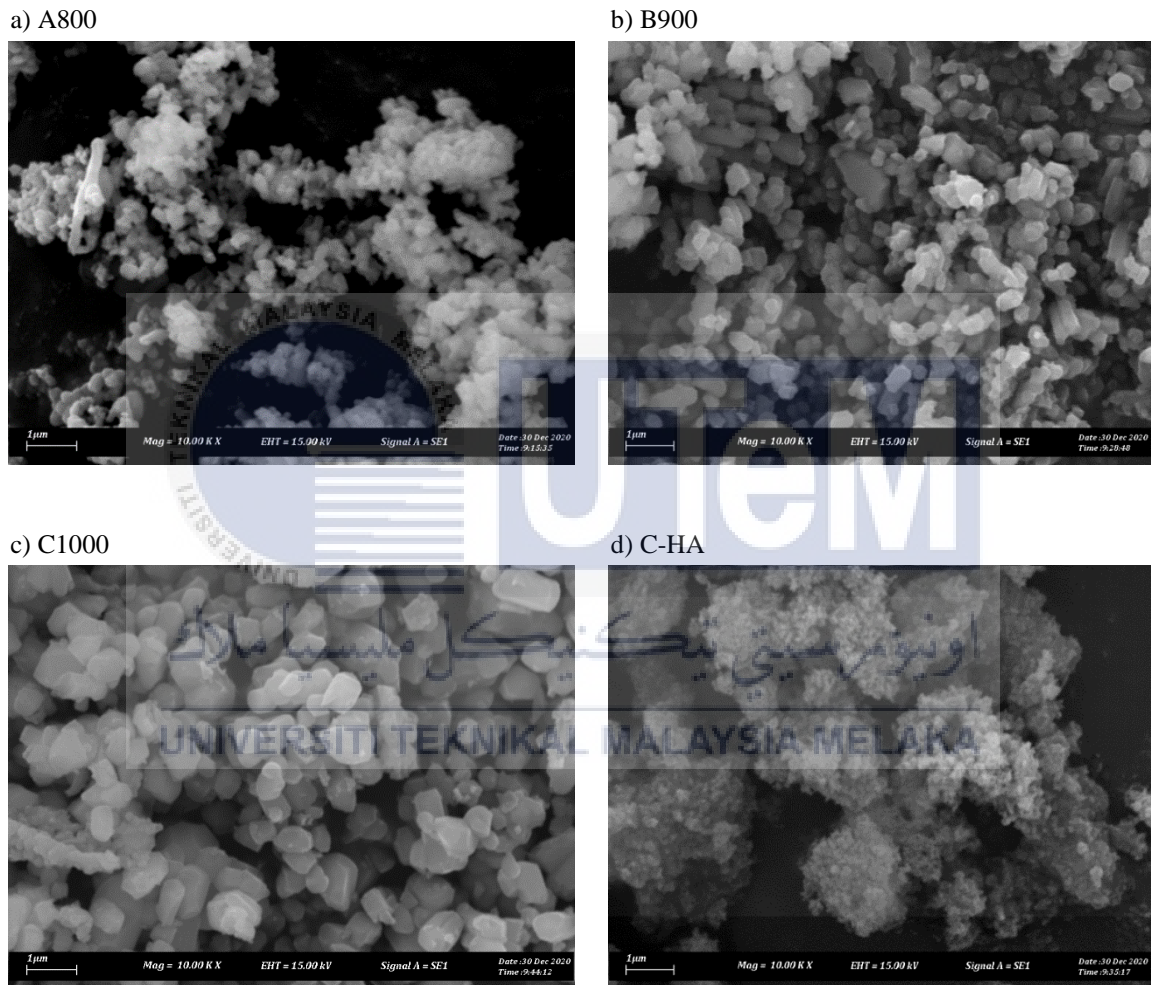


Figure 4.7: SEM images analysis of synthetic HA powders at calcined temperatures: a) 800°C (A800), b) 900°C (B900), c) 1000°C (C1000), d) Commercial HA (C-HA) at 10,000X

## CHAPTER 5

### CONCLUSION AND RECOMMENDATION

#### 5.1 Conclusion

*Skipjack tuna* bones were successfully used to produce hydroxyapatite (HA) using this thermal method. The synthesised HA was calcined and characterised its physical, chemical and mechanical properties. The characterisation of HA is depends on the effect of calcined temperature of initial solution. The results indicated that synthetic HA was completely formed where the XRD pattern show major HA-corresponding reflections and fewer CaP-reflections. From the XRD pattern, the highest intensity peak detected at  $32.15^\circ$  of calcined temperature  $1000^\circ\text{C}$ .

The second objective of this study are to characterise and analyse the physical, chemical and mechanical properties of fishbone. It was observed that the colour changes from yellow to white indicated the removal of collagen and other organic materials. Based on chemical properties, the FTIR analysis shows the stretching frequencies of raw fishbone are broader than calcined powder due to the presence of water, alkanes elements and carboxylic acid. The XRD analysis prove that the crystallite size of the sample is increase with the sharpness and the intensity increase of the XRD peaks when the temperature is increased. Besides that, all the HA samples consist of  $\text{PO}_4^{3-}$  chemical group, and only sample at  $800^\circ\text{C}$  consists of  $\text{CO}_3^{2-}$  chemical group as because the sample is prepared with different calcination temperature. The Vickers hardness of the sample increased rapidly from 0.55 GPa to 0.64 GPa when the calcination temperature increase. The hardness values also shows the synthetic HA from fishbone are in the range of actual human femoral cortical bone that in range of 0.3-0.6 GPa. The microstructure and morphology of HA is in agglomerated condition. It shows the relationship between the microstructure and the temperature. As the calcined temperature increases, HA particle was forming a dense particle and resulted in

increased particle size. Hence, it is concluded that 1000°C is the suitable calcination temperature with constant time for fishbone to obtain synthetic hydroxyapatite. This study shows that it is possible to recycle fishbone waste where it can be used in biomedicine and other potential applications.

## 5.2 Recommendation

After gone through this study, there are few recommendations suggested to call attention to the important aspect need to be focus about synthetic hydroxyapatite in the future. The significant recommendations for this objective as follows:

1. The study focused on the chemical composition of the sample. As to elucidate the impurity of these samples by observing the Ca/P atomic ratio, an elemental analysis using an EDX analysis is needed. EDX is versatility and potential for qualitative and quantitative analysis of the composition of the sample. This may help to improve the understanding of the heat treatment process that has affected the impurity of the sample.
2. The XRD analysis should be performed by comparing the experimental studies with commercial HA at different temperatures as well as synthetic HA from fishbone in order to obtain accurate results in terms of peak and HA intensity.
3. The morphology analysis was done using SEM and the image obtained was less distinct. However, the image can be enhanced using FESEM as it can obtained focus image for the result.

## 5.3 Sustainability Element

This research was motivated by innovation in the use of waste products producing synthetic hydroxyapatite for bone implants. In fact, the development of synthetic hydroxyapatite from fishbone waste with improved characteristics is a practical, economical process and an environmentally friendly synthesis method for large-scale production. As the



quality and purity of the product are almost the same as commercial HA, the use of waste materials can lower the cost of the synthesis material.

The data and results obtained can contribute to society in many ways, particularly in the field of biomedical and material engineering today. This study is very useful because it involves the management of organic waste and the use of fishbone for a variety of products to meet the needs of society. This study also reduces environmental problems, such as land pollution, for society. The benefit of this study is that the company will be exposed to the value of fishbone that can develop medical value material and the process of developing synthetic fishbone hydroxyapatite through the cleaning and heat treatment process.

#### **5.4 Life Long Learning Element**

In terms of basic characteristics and areas of practise, lifelong learning is an important strategy to individual development. This can lead to a positive contribution to the economy. The recovery of waste by-products for the production of valuable compounds is a method that has become more popular in recent years. The increase in the amount of waste is leading to disposal. As a result, there is a great potential for them to be used as a source of the compound to be marketed.

#### **5.5 Complexity Element**

This study is concerned with the complex decision making process. The complexity element applied in this study is the hardness test. Hardness is known as the resistance of material to localise the plastic deformation. Hardness ranges from very hard materials, ceramic, hard and soft metals and plastic. Toughness and strength is the mechanical properties need to be considered in this hardness test where hard material tend to have low toughness and easily to fracture. The temperature of the material need to be considered during experiment as the hardness value will decrease when the temperature of material is increase. Besides, drastic changes in hardness value will occur and will obtain impossible value of hardness test.

## REFERENCES

- Afriani, F., Tiandho, Y., Evi, J., Indriawati, A., & Rafsanjani, R. A. (2019, October). Synthesis and characterization of hydroxyapatite/silica composites based on cockle shells waste and tin tailings. In IOP Conference Series: Earth and Environmental Science (Vol. 353, No. 1, p. 012032). IOP Publishing.
- Alif, M. F., Aprillia, W., & Arief, S. (2017, November). Peat water purification by hydroxyapatite (HAp) synthesized from waste pensil (Corbicula molckiana) shells. In International Conference on Chemistry and Material Science (IC2MS), Malang Indonesia (pp. 1-6).
- Artioli, G., & Angelini, I. (2010). Scientific methods and cultural heritage: an introduction to the application of materials science to archaeometry and conservation science. Oxford University Press.
- Asri, R. I. M., Harun, W. S. W., Hassan, M. A., Ghani, S. A. C., & Buyong, Z. (2016). A review of hydroxyapatite-based coating techniques: Sol-gel and electrochemical depositions on biocompatible metals. *Journal of the mechanical behavior of biomedical materials*, 57, 95-108.
- Ayatollahi, M. R., Yahya, M. Y., Shirazi, H. A., & Hassan, S. A. (2015). Mechanical and tribological properties of hydroxyapatite nanoparticles extracted from natural bovine bone and the bone cement developed by nano-sized bovine hydroxyapatite filler. *Ceramics International*, 41(9), 10818-10827.
- Barakat, N. A., Khalil, K. A., Sheikh, F. A., Omran, A. M., Gaihre, B., Khil, S. M., & Kim, H. Y. (2008). Physicochemical characterizations of hydroxyapatite extracted from

bovine bones by three different methods: extraction of biologically desirable HAp. *Materials Science and Engineering: C*, 28(8), 1381-1387.

Basirun, W. J., Nasiri-Tabrizi, B., & Baradaran, S. (2018). Overview of hydroxyapatite–graphene nanoplatelets composite as bone graft substitute: mechanical behavior and in-vitro biofunctionality. *Critical Reviews in Solid State and Materials Sciences*, 43(3), 177-212.

Bluemel, J., Korte, S., Schenck, E., & Weinbauer, G. (Eds.). (2015). *The nonhuman primate in nonclinical drug development and safety assessment*. Academic Press.

Bigi, A., Boanini, E., Capuccini, C., & Gazzano, M. (2007). Strontium-substituted hydroxyapatite nanocrystals. *Inorganica Chimica Acta*, 360(3), 1009-1016.

Boniface, B., Albat, S., Tanakinjal, G. H., & Komilus, C. F. (2018). Determinants of trust and business performance: the case of tuna fishery industry in Semporna, Sabah. *International Food Research Journal*, 25.

Cahyanto, A., Kosasih, E., Aripin, D., & Hasratiningsih, Z. (2017, February). Fabrication of hydroxyapatite from fishbones waste using reflux method. In *IOP Conference Series: Materials Science and Engineering* (Vol. 172, No. 1, p. 012006). IOP Publishing.

Chalisserry, E. P., Nam, S. Y., Venkatesan, J., & Anil, S. (2018). Isolation and Characterization of Nanorod-Shaped Crystalline Hydroxyapatite from Parrotfishbone. *Journal of Biomaterials and Tissue Engineering*, 8(4), 473-481.

Chandler, H. (1999). *Introduction to hardness testing*. Hardness testing. USA: ASM International, 1-13.

Choudhary, O. P., & Choudhary, P. (2017). Scanning electron microscope: advantages and disadvantages in imaging components. *Int. J. Curr. Microbiol. Appl. Sci*, 6, 1877-1882.

- Dhamoon, R. K., Popli, H., Aggarwal, G., & Gupta, M. (2018). Particle size characterization techniques, factors and quality-by-design approach. *Int J Drug Deliv*, 10, 1-11.
- Diaz-Terán, J., Nevskaja, D. M., Fierro, J. L. G., López-Peinado, A. J., & Jerez, A. (2003). Study of chemical activation process of a lignocellulosic material with KOH by XPS and XRD. *Microporous and mesoporous materials*, 60(1-3), 173-181.
- Ding, D., Du, B., Zhang, C., Zaman, F., & Huang, Y. (2019). Isolation and identification of an antioxidant collagen peptide from skipjack tuna (*Katsuwonus pelamis*) bone. *RSC advances*, 9(46), 27032-27041.
- Earl, J. S., Wood, D. J., & Milne, S. J. (2006). Hydrothermal synthesis of hydroxyapatite. In *Journal of Physics: Conference Series* (Vol. 26, No. 1, p. 268). IOP Publishing.
- Eliaz, N., & Metoki, N. (2017). Calcium phosphate bioceramics: a review of their history, structure, properties, coating technologies and biomedical applications. *Materials*, 10(4), 334.
- Elliott, J. C. (2013). *Structure and chemistry of the apatites and other calcium orthophosphates*. Elsevier.
- Ghiasi, B., Sefidbakht, Y., & Rezaei, M. (2019). Hydroxyapatite for biomedicine and drug delivery. In *Nanomaterials for Advanced Biological Applications* (pp. 85-120). Springer, Cham.
- Gomes, D. S., Santos, A. M. C., Neves, G. A., & Menezes, R. R. (2019). A brief review on hydroxyapatite production and use in biomedicine. *Cerâmica*, 65(374), 282-302.
- Haider, A., Haider, S., Han, S. S., & Kang, I. K. (2017). Recent advances in the synthesis, functionalization and biomedical applications of hydroxyapatite: a review. *Rsc Advances*, 7(13), 7442-7458.

- Hariani, P. L., Muryati, M., Said, M., & Salni, S. (2020). Synthesis of Nano-Hydroxyapatite from Snakehead (*Channa striata*) Fishbone and its Antibacterial Properties. In *Key Engineering Materials* (Vol. 840, pp. 293-299). Trans Tech Publications Ltd.
- Hickey, D. J., Ercan, B., Sun, L., & Webster, T. J. (2015). Adding MgO nanoparticles to hydroxyapatite–PLLA nanocomposites for improved bone tissue engineering applications. *Acta biomaterialia*, 14, 175-184.
- Horvath, A. L. (2006). Solubility of structurally complicated materials: II. Bone. *Journal of physical and chemical reference data*, 35(4), 1653-1668.
- Hsieh, M. F., Perng, L. H., Chin, T. S., & Perng, H. G. (2001). Phase purity of sol–gel-derived hydroxyapatite ceramic. *Biomaterials*, 22(19), 2601-2607.
- Hosseinzadeh, E., Davarpanah, M., Nemati, N. H., & Tavakoli, S. A. (2014). Fabrication of a hard tissue replacement using natural hydroxyapatite derived from bovine bones by thermal decomposition method. *International journal of organ transplantation medicine*, 5(1), 23.
- Jang, H. L., Lee, H. K., Jin, K., Ahn, H. Y., Lee, H. E., & Nam, K. T. (2015). Phase transformation from hydroxyapatite to the secondary bone mineral, whitlockite. *Journal of Materials Chemistry B*, 3(7), 1342-1349.
- Jillavenkatesa, A., & Condrate Sr, R. A. (1998). Sol–gel processing of hydroxyapatite. *Journal of materials science*, 33(16), 4111-4119.
- Jonasz, M., & Fournier, G. R. (2007). General features of scattering of light by particles in water. *Light scattering by particles in water*, 87-143.
- Joseph, L., Jun, B. M., Flora, J. R., Park, C. M., & Yoon, Y. (2019). Removal of heavy metals from water sources in the developing world using low-cost materials: A review. *Chemosphere*, 229, 142-159.

- Kaflak, A., Moskalewski, S., & Kolodziejcki, W. (2019). The solid-state proton NMR study of bone using a dipolar filter: apatite hydroxyl content versus animal age. *RSC advances*, 9(29), 16909-16918.
- Khandelwal, H., & Prakash, S. (2016). Synthesis and characterization of hydroxyapatite powder by eggshell. *Journal of Minerals and Materials Characterization and Engineering*, 4(2), 119-126.
- Kashkarov, V. M., Goloshchapov, D. L., Rumyantseva, A. N., Seregin, P. V., Domashevskaya, E. P., Spivakova, I. A., & Shumilovich, B. R. (2011). X-ray diffraction and IR spectroscopy investigation of synthesized and biogenic nanocrystalline hydroxyapatite. *Journal of Surface investigation. x-ray, Synchrotron and Neutron Techniques*, 5(6), 1162-1167.
- Khiri, M. Z. A., Matori, K. A., Zaid, M. H. M., Abdullah, C. A. C., Zainuddin, N., Alibe, I. M., & Wahab, S. A. A. (2019). The effect of the Ph values and sintering temperatures on the physical, structural and mechanical properties of nano hydroxyapatite derived from ark clam shells (*Anadara granosa*) prepared via the wet chemical precipitate method. *Ceramics–Silikáty*, 63(2), 194-203.
- Kołodziejcka, B., Kaflak, A., & Kolmas, J. (2020). Biologically Inspired Collagen/Apatite Composite Biomaterials for Potential Use in Bone Tissue Regeneration—A Review. *Materials*, 13(7), 1748.
- Laskus, A., & Kolmas, J. (2017). Ionic substitutions in non-apatitic calcium phosphates. *International journal of molecular sciences*, 18(12), 2542.
- Levine, S. P., Li-Shi, Y., Strang, C. R., & Hong-Kui, X. (1989). Advantages and disadvantages in the use of Fourier Transform Infrared (FTIR) and filter infrared (FIR) spectrometers for monitoring airborne gases and vapors of industrial hygiene concern. *Applied Industrial Hygiene*, 4(7), 180-187.

- Lin, K., Chang, J. (2015). Structure and properties of hydroxyapatite for biomedical applications. In: (Ed.). Hydroxyapatite (HAp) for biomedical applications: Elsevier, p.3-19.
- Liu, Q., Huang, S., Matinlinna, J. P., Chen, Z., & Pan, H. (2013). Insight into biological apatite: physicochemical properties and preparation approaches. *BioMed research international*.
- Ma, G. (2019). Three common preparation methods of hydroxyapatite. *IOP Conference Series: Materials Science and Engineering*, IOP Publishing, p.033057.
- Martín, C., Kostarelos, K., Prato, M., & Bianco, A. (2019). Biocompatibility and biodegradability of 2D materials: graphene and beyond. *Chemical Communications*, 55(39), 5540-5546.
- Mirzaali, M. J., Schwiedrzik, J. J., Thaiwichai, S., Best, J. P., Michler, J., Zysset, P. K., & Wolfram, U. (2016). Mechanical properties of cortical bone and their relationships with age, gender, composition and microindentation properties in the elderly. *Bone*, 93, 196-211.
- Mouiya, M., Bouazizi, A., Abourriche, A., El Khessaimi, Y., Benhammou, A., Taha, Y., ... & Hannache, H. (2019). Effect of sintering temperature on the microstructure and mechanical behavior of porous ceramics made from clay and banana peel powder. *Results in Materials*, 4, 100028.
- Mustafa, N., Ibrahim, M. H. I., Asmawi, R., & Amin, A. M. (2015). Hydroxyapatite extracted from waste fishbones and scales via calcination method. In *Applied Mechanics and Materials* (Vol. 773, pp. 287-290). Trans Tech Publications Ltd.
- Nawang, R., Hussein, M. Z., Matori, K. A., Abdullah, C. A. C., & Hashim, M. (2019). Physicochemical properties of hydroxyapatite/montmorillonite nanocomposite prepared by powder sintering. *Results in Physics*, 15, 102540.

- Neacsu, I. A., Stoica, A. E., Vasile, B. S., & Andronescu, E. (2019). Luminescent hydroxyapatite doped with rare earth elements for biomedical applications. *Nanomaterials*, 9(2), 239.
- Obada, D. O., Dauda, E. T., Abifarin, J. K., Dodoo-Arhin, D., & Bansod, N. D. (2020). Mechanical properties of natural hydroxyapatite using low cold compaction pressure: Effect of sintering temperature. *Materials Chemistry and Physics*, 239, 122099.
- Pal, A., Paul, S., Choudhury, A. R., Balla, V. K., Das, M., & Sinha, A. (2017). Synthesis of hydroxyapatite from Lates calcarifer fishbone for biomedical applications. *Materials Letters*, 203, 89-92.
- Pokhrel, S. (2018). Hydroxyapatite: preparation, properties and its biomedical applications. *Advances in Chemical Engineering and Science*, 8(04), 225.
- Pornchaloempong, P., Sirisomboon, P., & Nunak, N. (2012). Mass-volume-area properties of frozen skipjack tuna. *International Journal of Food Properties*, 15(3), 605-612.
- Pu'ad, N. M., Koshy, P., Abdullah, H. Z., Idris, M. I., & Lee, T. C. (2019). Syntheses of hydroxyapatite from natural sources. *Heliyon*, 5(5), e01588.
- Ramesh, S., Loo, Z. Z., Tan, C. Y., Chew, W. K., Ching, Y. C., Tarlochan, F., & Sarhan, A. A. (2018). Characterization of biogenic hydroxyapatite derived from animal bones for biomedical applications. *Ceramics International*, 44(9), 10525-10530.
- Razali, N. M., Pramanik, S., Osman, N. A., Radzi, Z., & Pinguan-Murphy, B. (2016). Conversion of calcite from cockle shells to bioactive nanorod hydroxyapatite for biomedical applications. *J. Ceram. Process. Res*, 17, 699-706.
- Rhee, S. H. (2002). Synthesis of hydroxyapatite via mechanochemical treatment. *Biomaterials*, 23(4), 1147-1152.



- Sadat-Shojai, M., Atai, M., & Nodehi, A. (2011). Design of experiments (DOE) for the optimization of hydrothermal synthesis of hydroxyapatite nanoparticles. *Journal of the Brazilian Chemical Society*, 22(3), 571-582.
- Sahu, S., Mehra, D., & Agarwal, R. D. (2012). Characterization and Thermal Analysis of Hydroxyapatite Bioceramic Powder Synthesized by Sol-Gel Technique. *Biomaterials for Spinal Surgery*, 281-289.
- Samsudin, B., Sallehudin, J., Effarina, M. F., & Nor Azlin, M. (2015). Malaysia national report to the scientific committee of the Indian Ocean tuna commission for 2015. Information on fisheries, research and statistics-2016-SC19-NR16.
- Santos, M. H., Oliveira, M. D., Souza, L. P. D. F., Mansur, H. S., & Vasconcelos, W. L. (2004). Synthesis control and characterization of hydroxyapatite prepared by wet precipitation process. *Materials Research*, 7(4), 625-630.
- Saxena, V., Hasan, A., & Pandey, L. M. (2018). Effect of Zn/ZnO integration with hydroxyapatite: a review. *Materials technology*, 33(2), 79-92.
- Shi, P., Liu, M., Fan, F., Yu, C., Lu, W., & Du, M. (2018). Characterization of natural hydroxyapatite originated from fishbone and its biocompatibility with osteoblasts. *Materials Science and Engineering: C*, 90, 706-712.
- Silva, C. C., Pinheiro, A. G., Miranda, M. A. R., Góes, J. C., & Sombra, A. S. B. (2003). Structural properties of hydroxyapatite obtained by mechanosynthesis. *Solid state sciences*, 5(4), 553-558.
- Suguna, J. (2019). Synthesis of hydroxyapatite from fishbone (scomber scombrus) using thermal decomposition method/Suguna Jeganathan (Doctoral dissertation, University of Malaya).
- Sun, R. X., Lv, Y., Niu, Y. R., Zhao, X. H., Cao, D. S., Tang, J., & Chen, K. Z. (2017). Physicochemical and biological properties of bovine-derived porous

hydroxyapatite/collagen composite and its hydroxyapatite powders. *Ceramics International*, 43(18), 16792-16798.

Sunil, B. R., & Jagannatham, M. (2016). Producing hydroxyapatite from fishbones by heat treatment. *Materials Letters*, 185, 411-414.

Suseno, S. H., Hidayat, T., Paramudhita, P. S., Ekawati, Y., & Arifianto, T. B. (2015). Changes in nutritional composition of skipjack (*Katsuwonus pelamis*) due to frying process.

Szcześ, A., Hołysz, L., & Chibowski, E. (2017). Synthesis of hydroxyapatite for biomedical applications. *Advances in colloid and interface science*, 249, 321-330.

Tan, C., Mansor, S., Ibrahim, H., & Rashid, A. (2002). Studies of sea surface temperature and chlorophyll-a variations in east coast of peninsular malaysia. *Pertanika Journal of Science & Technology*, 10(1), 13-24.

Thirumalai, J. (Ed.). (2018). Hydroxyapatite: advances in composite nanomaterials, biomedical applications and its technological facets. BoD–Books on Demand.

Türk, S., Altınsoy, İ., Efe, G. Ç., Ipek, M., Özacar, M., & Bindal, C. (2019). Effect of solution and calcination time on sol-gel synthesis of hydroxyapatite. *Journal of Bionic Engineering*, 16(2), 311-318.

Upadhyay, R. K. (2017). Role of calcium bio-minerals in regenerative medicine and tissue engineering. *J. Stem Cell Res. Ther*, 2(00081.10), 15406.

Vallet-Regí, M., & Navarrete, D. A. (2015). Nanoceramics in clinical use: from materials to applications. Royal Society of Chemistry.

Veljović, Đ., Vuković, G., Steins, I., Palcevskis, E., Uskoković, P. S., Petrović, R., & Janačković, Đ. (2013). Improvement of the mechanical properties of spark plasma sintered hap bioceramics by decreasing the grain size and by adding multi-walled carbon nanotubes. *Science of Sintering*, 45(2), 233-243.

- Venkatesan, J., Lowe, B., Manivasagan, P., Kang, K. H., Chalisserry, E. P., Anil, S. & Kim, S. K. (2015). Isolation and characterization of nano-hydroxyapatite from salmon fishbone. *Materials*, 8(8), 5426-5439.
- Wagh, A. S. (2016). *Chemically bonded phosphate ceramics: twenty-first century materials with diverse applications*. Elsevier.
- Yang, Z., Fang, Z., Zheng, L., Cheng, W., Tsang, P. E., Fang, J., & Zhao, D. (2016). Remediation of lead contaminated soil by biochar-supported nano-hydroxyapatite. *Ecotoxicology and environmental safety*, 132, 224-230.
- Zainol, I., Adenan, N. H., Rahim, N. A., & Jaafar, C. A. (2019). Extraction of natural hydroxyapatite from tilapia fish scales using alkaline treatment. *Materials Today: Proceedings*, 16, 1942-1948.
- Zainuddin, M., Farhum, A., Safruddin, S., Selamat, M. B., Sudirman, S., Nurdin, N. & Saitoh, S. I. (2017). Detection of pelagic habitat hotspots for skipjack tuna in the Gulf of Bone-Flores Sea, southwestern Coral Triangle tuna, Indonesia. *PloS one*, 12(10), e0185601.
- Zeng, R., Tang, W., Ding, C., Yang, L., Gong, D., Kang, Z. & Wu, Y. (2019). Preparation of anionic-cationic co-substituted hydroxyapatite for heavy metal removal: Performance and mechanisms. *Journal of Solid State Chemistry*, 280, 120960.
- Zhang, X., & Vecchio, K. S. (2007). Hydrothermal synthesis of hydroxyapatite rods. *Journal of Crystal Growth*, 308(1), 133-140.
- Zhuofan, C., Baoxin, H., Haobo, P., & Darvell, B. W. (2009). Solubility of Bovine-Derived Hydroxyapatite by Solid Titration, pH 3.5– 5. *Crystal Growth and Design*, 9(6), 2816-2820.

## APPENDIX A

**APPENDIX A: Final Year Project 1 Schedule Gantt chart**

TASK NAME	FINAL YEAR PROJECT I (SEM 19/20)																			
	FEBRUARY				MARCH				APRIL				MAY				JUNE			
	W1	W2	W3	W4	W1	W2	W3	W4	W1	W2	W3	W4	W1	W2	W3	W4	W1	W2	W3	W4
<b>1) DEFINE: PROPOSAL STAGE</b>																				
Briefing FYP1																				
Find a supervisor																				
Project title selection																				
<b>2) MEASURE: INITIAL STAGE</b>																				
Study the problem statement																				
Identify project goals																				
Research literature review																				
Proposed and construct method																				
Survey required instruments																				
Study the expected result																				
Prepare for presentation																				
Presentation																				
<b>3) FINAL REPORT STAGE</b>																				
Final project report submission																				
Log book submission																				
<b>4) APPOINTMENT WITH SUPERVISOR</b>																				

## APPENDIX B

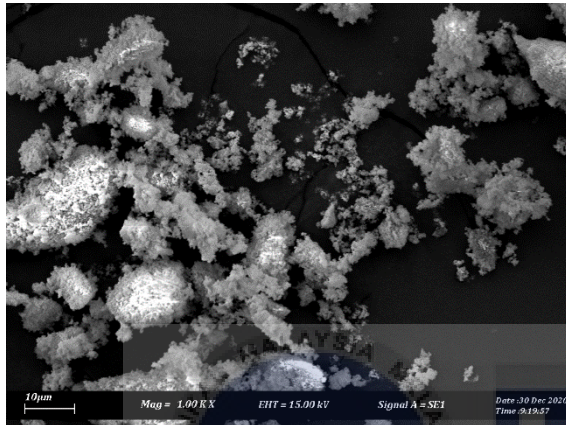
**Appendix B: Final Year Project 2 Schedule Gantt chart**

TASK NAME	FINAL YEAR PROJECT II (SEM 20/21)																			
	OCTOBER				NOVEMBER				DECEMBER				JANUARY				FEBRUARY			
	W1	W2	W3	W4	W1	W2	W3	W4	W1	W2	W3	W4	W1	W2	W3	W4	W1	W2	W3	W4
<b>1) METHODOLOGY</b>																				
Briefing FYPII																				
Amendment of FYPI																				
Prediction result																				
<b>2) RESULT AND DISCUSSION</b>																				
Preparing the dried fishbone																				
Calcination process																				
Crushing process																				
Preparation HA pellet																				
Sintering process																				
FTIR analysis																				
XRD analysis																				
Vickers hardness Test																				
SEM analysis																				
<b>3) FINAL REPORT STAGE</b>																				
Prepare for presentation																				
Presentation																				
Final project report submission																				
Log book submission																				
<b>4) APPOINTMENT WITH SUPERVISOR</b>																				

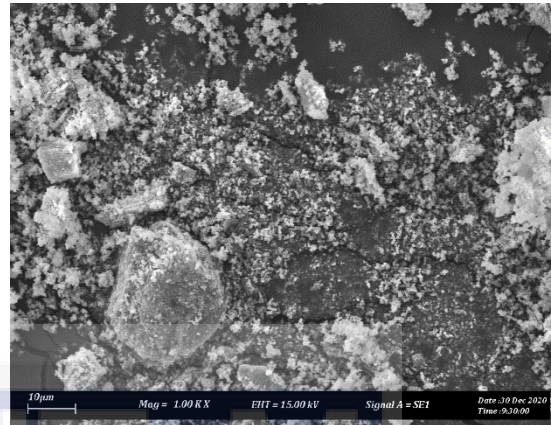
## APPENDIX C

### Appendix C: Scanning Electron Microscopy (SEM) Images

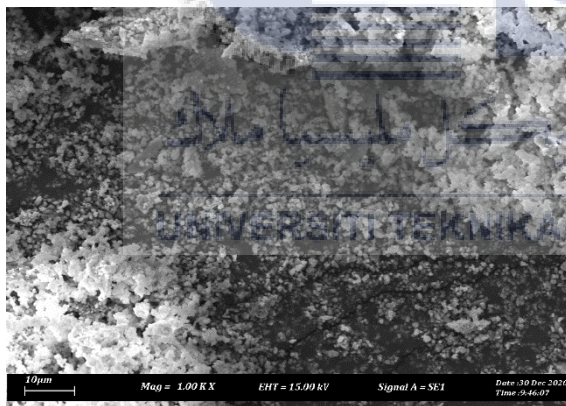
a) A800



b) B900



c) C1000



d) C-HA

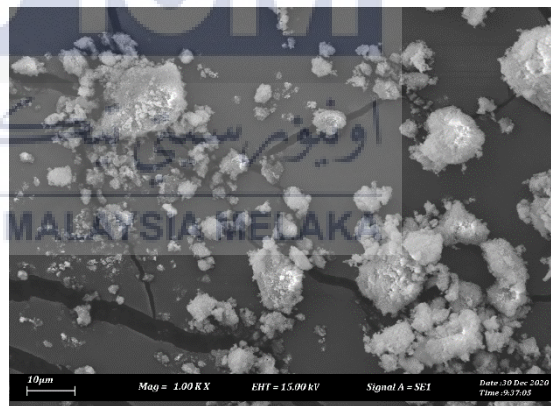
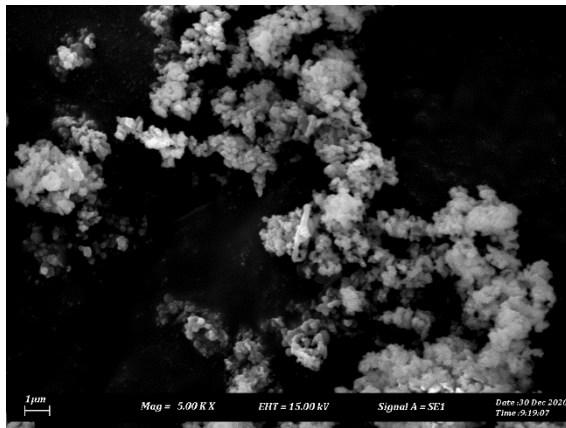


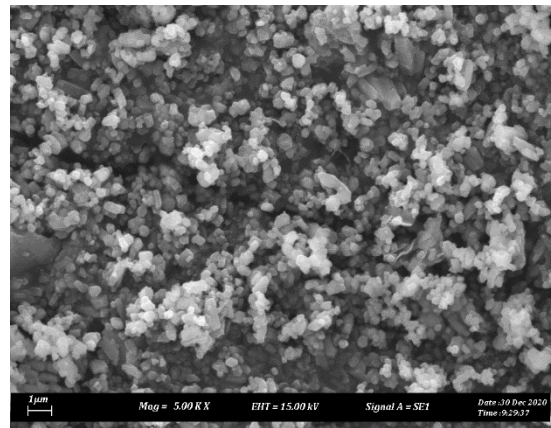
Figure 1: SEM images analysis of synthetic HA powders at calcined temperatures: a) 800°C (A800), b) 900°C (B900), c) 1000°C (C1000), d) Commercial HA (C-HA) at 1,000X



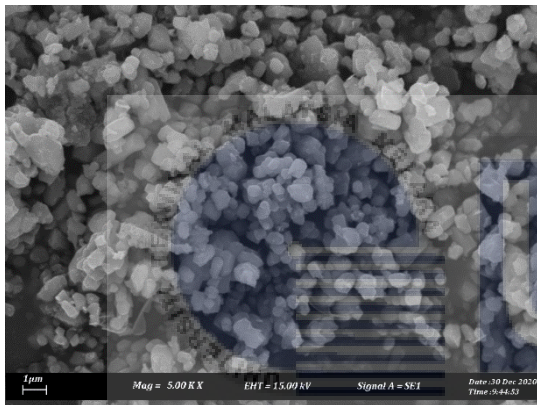
a) A800



b) B900



c) C1000



d) C-HA

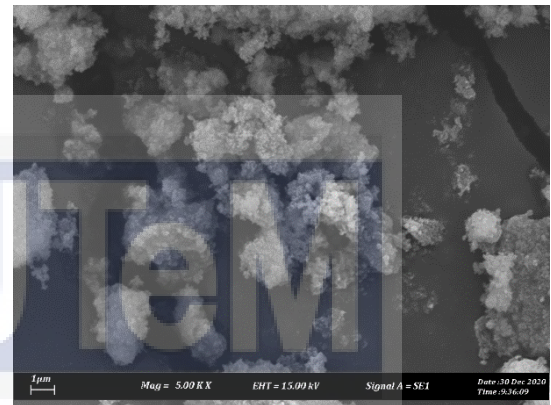


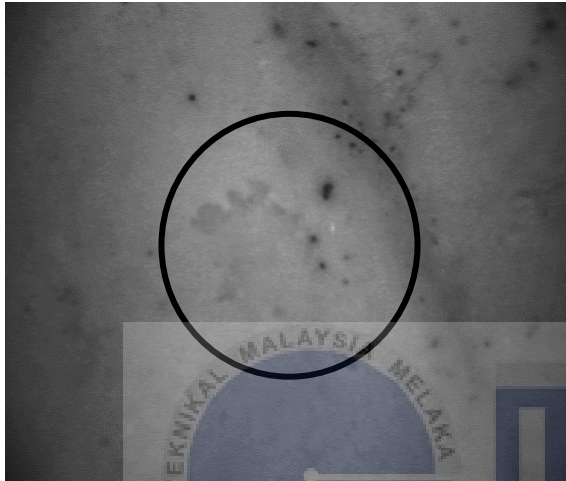
Figure 2: SEM images analysis of synthetic HA powders at calcined temperatures: a) 800°C (A800), b) 900°C (B900), c) 1000°C (C1000), d) Commercial HA (C-HA) at 5,000X

UNIVERSITI TEKNIKAL MALAYSIA MELAKA

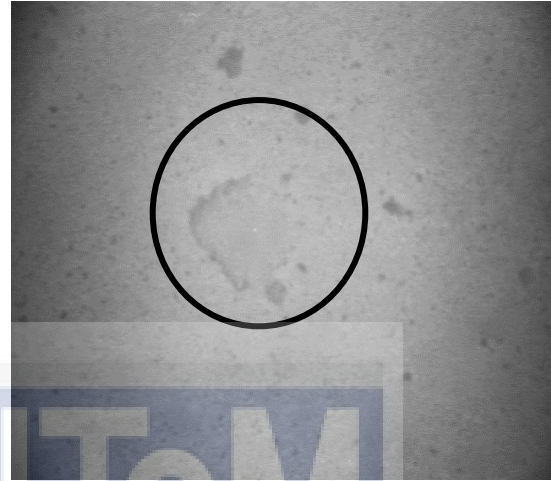
## APPENDIX D

### Appendix D: Vickers Hardness Images of Three Sample

a) A800



b) B900



c) C1000



Figure 3: Vickers hardness images analysis of synthetic HA pellet at calcined temperatures: a) 800°C (A800), b) 900°C (B900), c) 1000°C (C1000)